THE UNIVERSITY OF ALBERTA

DETERMINATION OF THE RATIO T_1/T_2 IN MULTILINE NMR SPECTRA

BY

© WILLIAM PUI YUEN HO

A THESIS

SUBMITTED TO THE FACULTY OF GRADUATE STUDIES AND RESEARCH

IN PARTIAL FULFILMENT OF THE REQUIREMENTS FOR THE DEGREE

OF

MASTER OF SCIENCE

DEPARTMENT OF CHEMISTRY

EDMONTON, ALBERTA

SPRING, 1979

TO MY MOTHER & MAGGIE

ABSTRACT

In complex multiline Fourier transform nuclear magnetic resonance spectra, the spin-lattice relaxation time, T_1, may be easily measured using the $180° - \tau - 90°$ pulse sequence (1). The spin-spin relaxation time, T_2, is not as accessible. The standard methods of measurement require selective excitation and precise pulse control (2).

An offset saturation technique has been developed which measures the ratio T_1/T_2 for lines in a multiline spectrum. The ratio is a sensitive probe of molecular dynamics; its value is usually more significant than those of the relaxation times themselves. This technique has been performed in both proton and carbon-13 FTNMR modes. An investigation into the motions of biologically significant molecules, such as adenosine 5'-triphosphate (ATP) and adenylyl (3'→5') adenosine (ApA), has been carried out using this method.

The measurement is simple and rapid, and does not involve critical control of the pulse sequence. In conjunction with a T_1 determination, it provides measurements of the T_2's of many resonances in a single session.

ACKNOWLEDGEMENTS

I would like to express my grateful thanks to my superviser, Dr. John S. Martin, for his guidance and help during the course of this research. I am also indebted to the following people:

Dr. Alex Bain who originally proposed this research topic.

Dr. George Kotowycz for his comments and suggestions.

Dr. Tom Nakashima and Mr. Glen Bigam for their valuable help and advice.

TABLE OF CONTENTS

LIST OF TABLES

LIST OF FIGURES

CHAPTER ONE

INTRODUCTION

The last two decades have witnessed an ever increasing utilization of NMR relaxation techniques for the study of molecular motions (3,4). The characterization of motion solely by spin-lattice relaxation time studies requires relaxation measurements to be made corresponding to both high and low frequency regions of the spectral density of the motion in question; that is, in the region

$$\omega_o \tau_c << 1 \qquad [1]$$

as well as in the "extreme narrowing" region

$$\omega_o \tau_c >> 1 \qquad [2]$$

where τ_c is the correlation time of the motion and ω_o is the Larmor frequency. In principle, one may vary temperature or magnetic field strength to satisfy the criteria expressed in equations [1] and [2]. In practice, more often than not, the use of these methods is limited.

Since the introduction of commercial Fourier transform NMR, measurement of spin-lattice relaxation times has become a somewhat routine method of studying molecular structure and motion. However, T_1's are sensitive only to rapid motions with frequency components on the order of the Larmor frequency. More complete information is available if something is known about the low frequency compon-

ents of the molecular motion. Consequently, there has been an effort to develop a method to measure T_2's by FTNMR (5,6). The theory of spin-lattice relaxation in the rotating frame ($T_{1\rho}$) has been well developed (7,8). It provides similar information to T_2.

With the exception of T_2 data obtained from linewidth measurements, neither T_2 nor $T_{1\rho}$ techniques (9) have been commonly employed on multiline spectra. The reason for this is due, at least in part, to the difficulty of performing and interpreting these experiments.

Based on the steady state solution of the Bloch equations with the assumption of a saturation factor greater than unity, a simple offset saturation technique of determining the ratio T_1/T_2 has been developed. It can be performed on any FTNMR spectrometer capable of homonuclear Overhauser or gated decoupling experiments. Nearby signals do not interfere; in fact, in a dense spectrum it is possible to get relaxation data for many neighbouring resonances in a single run. The only restrictions in this context are that nearby spins are not coupled nor may they relax each other. This condition is met by many systems of interest: for example, by the histidine and nitrogen base protons which appear at the low shielding end of spectra of biologically interesting molecules.

Samples of water at pH 11.5 and chloroform were used to demonstrate the technique. The coupling between the

chloroform hydrogen and chlorine is also calculated from the relaxation times obtained by the offset saturation experiment. This technique has been applied to explore the internal motions, conformations and base-stacking of adenosine 5'-triphosphate and adenylyl (3'→5') adenosine molecules. Finally, an application of the offset saturation technique was made in the carbon-13 FTNMR mode on the resonances of *ortho*-dichlorobenzene.

CHAPTER TWO

THEORY

The most commonly employed procedure for measuring spin-lattice relaxation times is the 180°-τ-90° pulse sequence. In this method, a 180° pulse inverts the magnetization along the z' axis (Figure 1-a). After some time τ, during which the partial relaxation has occurred (Figure 1-b), a 90° pulse is applied. This rotates the magnetization vector into the y' axis (or -y' axis depending upon the relative length of τ) and a free induction decay (FID) signal results. This pulse program has made it possible to determine simultaneously the T_1's of many nuclei in a dense, complex spectrum.

No method comparable in utility and convenience exists for the evaluation of spin-spin relaxation time, T_2. Only in the case of very large molecules with long correlation times can T_2 be obtained from a linewidth measurement. The standard spin-spin relaxation time measurement is based on Hahn's spin-echo technique (10). In this method, careful control of pulse parameters is needed. The requirement of a highly stable field - frequency ratio has been pointed out by Freeman and Hill (11), and errors due to neglect of diffusion have been discussed by Allerhand *et al* (12). The effects of instabilities of pulse widths and pulse intervals have been analyzed by Weiss (13). In view of the wealth of possible errors which may arise from the above

sources, it is not surprising that spin-spin relaxation time determinations are not as commonly reported as spin-lattice relaxation times.

Measurement of either the spin-spin relaxation time or of the ratio T_1/T_2 is essential to the study of molecular dynamics. Common to all relaxation processes is the kind of behaviour shown in Figure 2. Both T_1 and T_2 are determined by two factors: the strength of stochastic interaction, and its correlation times, τ_c. The correlation time dependences differ outside the region of extreme narrowing - that is, when the correlation time is comparable to or greater than the inverse of the spectrometer frequency. Initially T_1 and T_2 decrease as molecular motion slows up until the limit of $2\pi\nu_o\tau_c = 1$ is reached, after which T_1 increases and T_2 decreases further.

In this useful domain, the ratio of the relaxation times is independent of the strength of the interaction. The general equations describing nuclear relaxation resulting from random molecular motion will be of the form (14)

$$\frac{1}{T_1} \propto \bar{b}^2{}_{loc}\left[\frac{c_1\tau_c}{1 + 4\pi^2\nu^2\tau_c{}^2}\right] \qquad [3]$$

$$\frac{1}{T_2} \propto \bar{b}^2{}_{loc}\left[c_2\tau_c + \frac{c_3\tau_c}{1 + 4\pi^2\nu^2\tau_c{}^2}\right] \qquad [4]$$

where

C_1, C_2, C_3 are constants

ν = Larmor frequency of a nucleus

τ_c = reorientational correlation time

b^2_{loc} = mean square average local magnetic field (the value and origin of b_{loc} will depend on the mechanism under consideration (Appendix 1).

If only a single mechanism is active, the relaxation times can yield the correlation time directly.

One of the correct treatments of the magnetic resonance phenomenon is that of Bloch (15,16). The equations describe the response of the net magnetization to continuous radio-frequency irradiation at some frequency ω near the resonant frequency ω_o. In order to discuss the equilibrium state of magnetization $\vec{M}$ in the presence of the static magnetic field $\vec{B}_0$ and the exciting field $\vec{B}_2$ in the FT experiment, one needs the steady state solution of the Bloch equations in the rotating frame. It is

$$u = M_o \frac{\gamma B_2 T_2^2 (\omega_o - \omega)}{1 + T_2^2(\omega_o-\omega)^2 + \gamma^2 B_2^2 T_1 T_2} \qquad [5]$$

$$v = M_o \frac{\gamma B_2 T_2}{1 + T_2^2(\omega_o-\omega)^2 + \gamma^2 B_2^2 T_1 T_2} \qquad [6]$$

$$M_z = M_o \frac{1 + T_2^2(\omega_o-\omega)^2}{1 + T_2^2(\omega_o-\omega)^2 + \gamma^2 B_2^2 T_1 T_2} \qquad [7]$$

where

ω_o = Larmor resonant frequency

B_2 = radio frequency magnetic field at angular frequency ω

γ = magnetogyric ratio

T_1 = spin-lattice relaxation time

T_2 = spin-spin relaxation time

In linear continuous-wave spectroscopy, the saturation factor, $\gamma B_2 \sqrt{T_1 T_2}$, is kept much smaller than unity. Under such conditions where $\gamma B_2 \sqrt{T_1 T_2} \ll 1$, that is, the radio-frequency power applied is sufficiently low that saturation does not occur, then further simplification takes place and the Bloch equations become

$$u = M_o \frac{\gamma B_2 T_2^2 (\omega_o - \omega)}{1 + T_2^2 (\omega_o - \omega)^2} \qquad [8]$$

$$v = M_o \frac{\gamma B_2 T_2}{1 + T_2^2 (\omega_o - \omega)^2} \qquad [9]$$

$$M_z = M_o \frac{1 + T_2^2 (\omega_o - \omega)^2}{1 + T_2^2 (\omega_o - \omega)^2} \qquad [10]$$

This can be seen to be a Lorentzian line centred at ω_o with a line width at half height of $1/\pi T_2$. The u mode is the associated dispersive component. Figure 3 illustrates the u and v mode signals. The amplitude of the

v mode signal below saturation is proportional to $\gamma B_2 T_2$ and it has a maximum when $\gamma^2 B_2{}^2 T_1 T_2$ equals unity.

The Bloch theory therefore predicts that NMR signal has two components which are 90° out of phase. The u mode component is in phase with the exciting field, that is, along the same axis; the v mode is out of phase with the excitation, that is, along the axis orthogonal to both the excitation and the static field. The Fourier transformation of a free induction decay of an equilibrium system also yields the u and v mode signals (17).

When considering the condition where the saturation factor, $\gamma B_2 \sqrt{T_1 T_2}$, is much larger than unity, the three components of magnetization in the steady state are shown in Figure 4. A limiting behaviour exists in which the absorption mode disappears, and the dispersion mode, u, and the z component, M_z, show characteristic patterns whose amplitudes are proportional to the equilibrium magnetization, M_0. The widths of these patterns are determined by the saturation factor and the relaxation times, and most important, are much greater than typical field inhomogeneities.

By rewriting the steady state Bloch equations, one gets

$$\frac{u}{M_o} = \frac{\gamma B_2 T_2^{\,2}(\omega_o-\omega)}{S}$$

$$= \frac{\gamma B_2\sqrt{T_1 T_2}\cdot T_2(\omega_o-\omega)\cdot\sqrt{T_2/T_1}}{S}$$

$$= \frac{f\ \sqrt{r}\ \ c}{1 + c^2 + f^2} = U \qquad [11]$$

$$\frac{v}{M_o} = \frac{\gamma B_2 T_2}{S}$$

$$= \frac{\gamma B_2\sqrt{T_1 T_2}\cdot\sqrt{T_2/T_1}}{s}$$

$$= \frac{f\ \sqrt{r}}{1 + c^2 + f^2} = V \qquad [12]$$

$$\frac{M_z}{M_o} = \frac{1 + T_2^{\,2}(\omega_o-\omega)^2}{s}$$

$$= \frac{1 + c^2}{1 + c^2 + f^2} = Z \qquad [13]$$

where

$$s = 1 + T_2^{\,2}(\omega_o - \omega)^2 + \gamma^2 B_2^{\,2} T_1 T_2$$

$$= 1 + c^2 + f^2$$

$$r = T_2/T_1$$

$$f = \text{saturation factor}$$

$$= \gamma B_2 \sqrt{T_1 T_2}$$

$$c = T_2(\omega_o - \omega)$$

In the event that $\gamma B_2 \sqrt{T_1 T_2} >> 1$, one obtains

$$z = \frac{M_z}{M_o} \qquad \frac{c^2}{c^2 + f^2} = z' \qquad [14]$$

$$u = \frac{u}{M_o} \qquad \frac{f \sqrt{r} \; c}{c^2 + f^2} = u' \qquad [15]$$

$$v = \frac{v}{M_o} \qquad \frac{f \sqrt{r}}{c^2 + f^2} = v' \qquad [16]$$

Equation [15] can be written as

$$\frac{u}{M_o} = \frac{\gamma B_2 T_2^{\,2} (\delta\omega)}{T_2^{\,2} (\delta\omega)^2 + \gamma^2 B_2^{\,2} T_1 T_2} \qquad [15a]$$

By setting the derivative of u/M_0 with respect to $\delta\omega$ to zero, one obtains,

$$(\delta\omega)_{\substack{max \\ min}} = \pm\ \gamma B_2 \sqrt{T_1/T_2} \qquad [17]$$

At $(\delta\omega)_{\substack{max \\ min}}$,

$$\frac{u}{M_o} = \frac{1}{2} \sqrt{T_2/T_1} \qquad [18]$$

As the strong field sweeps through resonance, the magnetization describes an ellipse in the xz plane. The result is shown in Figure 5. The residual v magnetization at resonance is of the order of $1/f$. The residual z magnetization, and the departure of its value from the approximate form, are both of the order of $1/f^2$. In order to observe the z component without the interference of u (and sometimes v) mode signals in the neighbourhood of resonance, clearly the saturation factor must be larger than 10 and preferably 100 or more.

The most useful component of magnetization to FTNMR spectroscopy is the z component. Figure 4(c) represents the steady state value of the normalized z component. If the saturation factor is large, from equation [14],

$$\frac{M_z}{M_o} = \frac{1}{1 + \dfrac{\gamma^2 B_2^{\,2}}{(\omega_o - \omega)^2} \cdot \dfrac{T_1}{T_2}} \qquad [19]$$

$$\frac{T_1}{T_2} = \left(\frac{\gamma B_2}{2\pi}\right)^{-2} (\Delta\nu)^2 \left(\frac{M_o}{M_z} - 1\right) \qquad [20]$$

The z component has a very simple frequency dependence. It goes to zero at resonance, and its departure from equilibrium shows a symmetric, Lorentzian behaviour. The width of the dip is determined in a very simple way by the strength of the irradiating field, B_2, and the ratio of the relaxation times, T_1/T_2. If this component can be followed as a function of the frequency offset of a strong irradiation, based on equation [20], a simple analysis can be used to yield the ratio of the relaxation times.

The full analysis of data and interpretation of results will be shown in the next section.

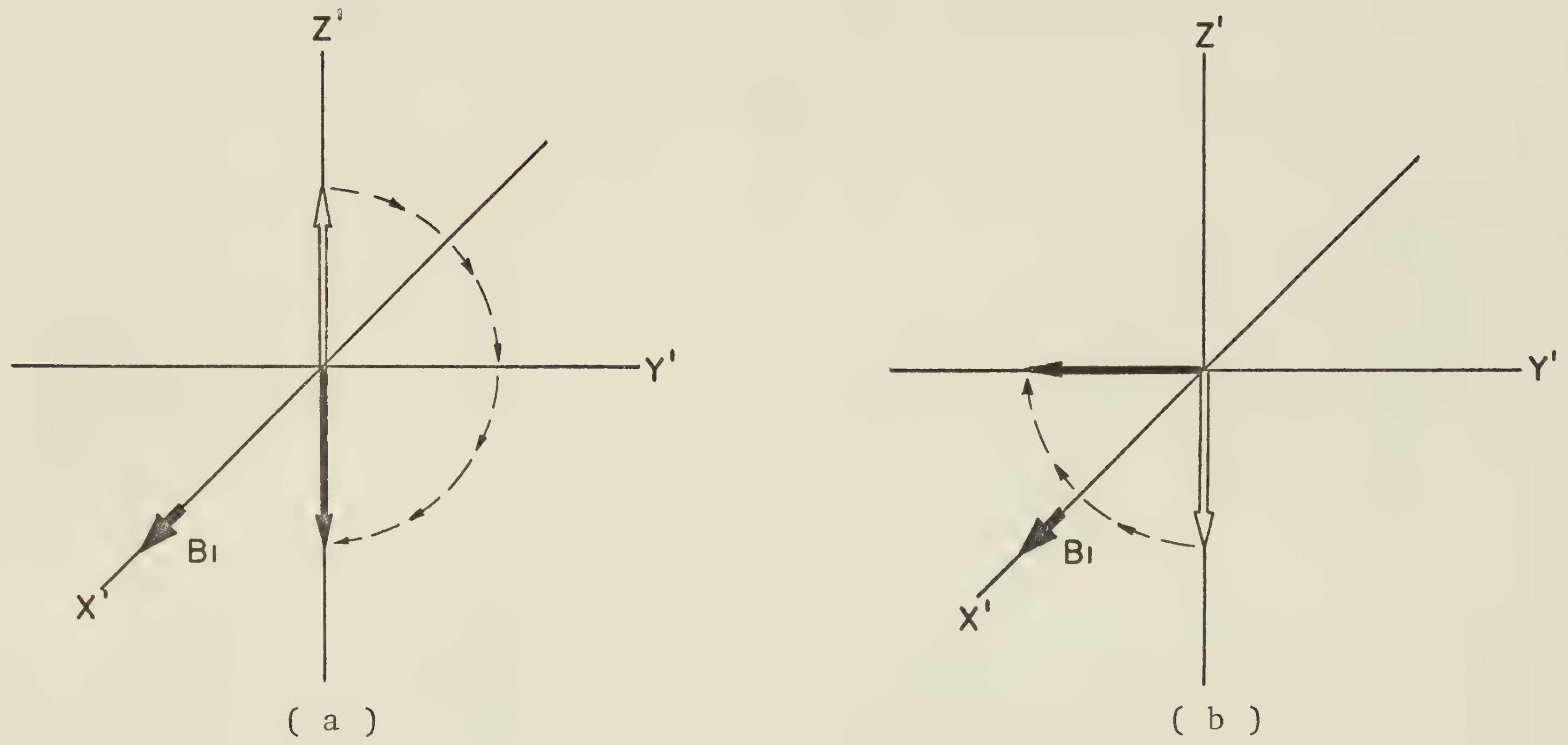

FIGURE 1: Determination of spin-lattice relaxation time in the rotating frame by (180^0 - τ - 90^0) pulse sequence. (a) The magnetization M is inverted by a 180^0 pulse at time 0. (b) After a time τ a 90^0 pulse rotates M to the y' (or -y') axis.

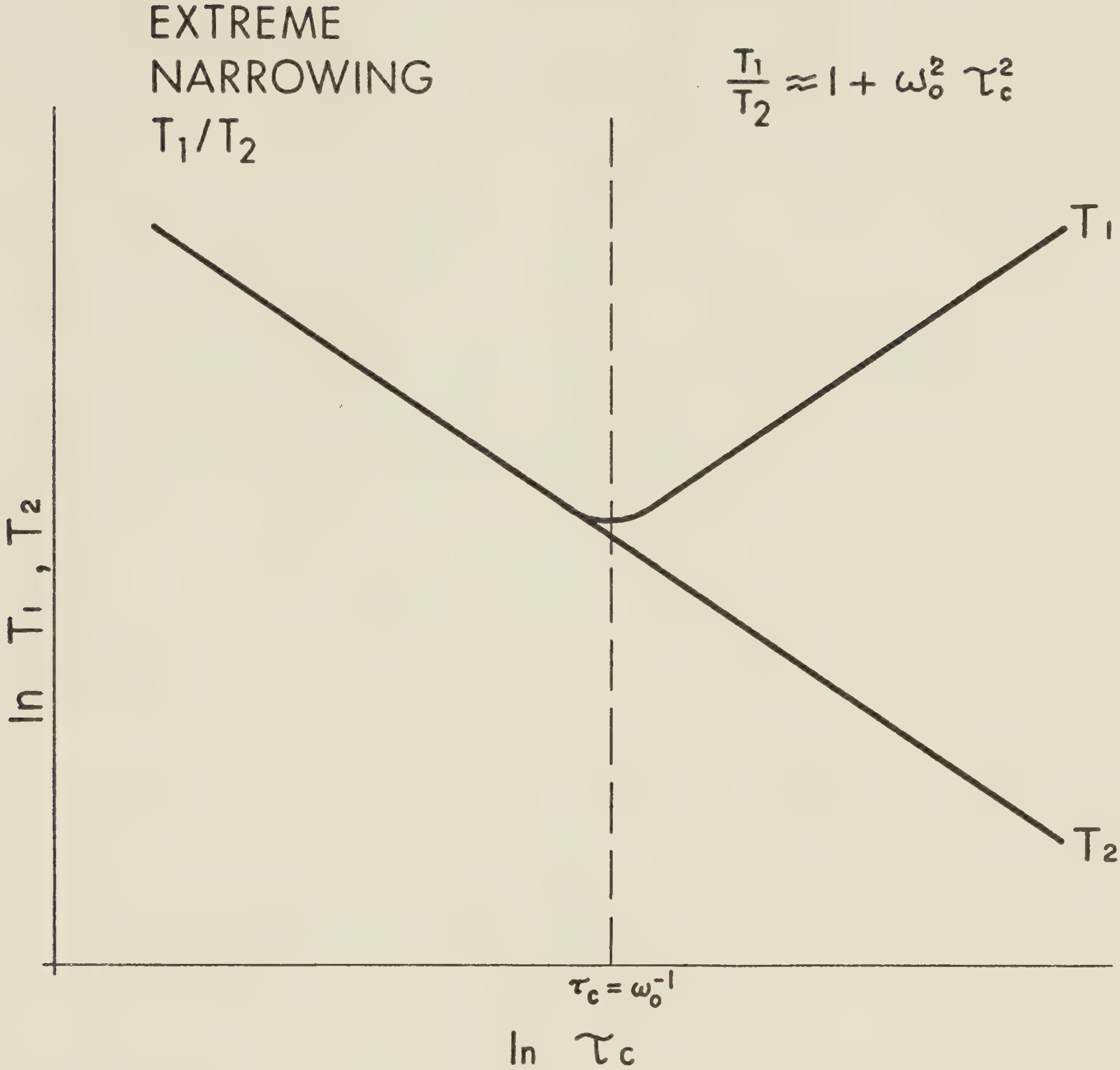

FIGURE 2: A log-log plot on the dependence of relaxation times on molecular correlation time, τ_c.

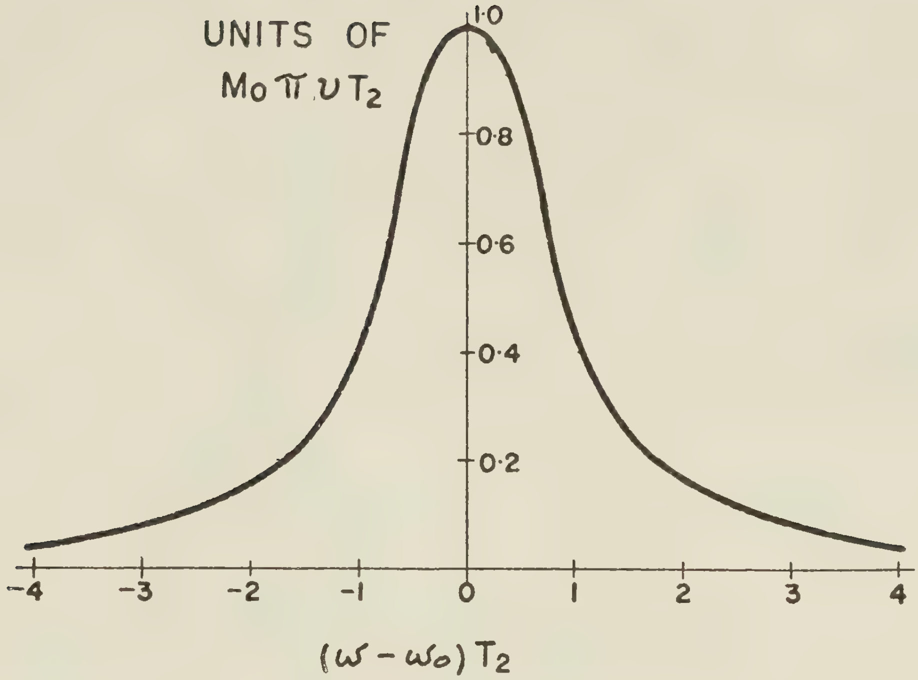

(a)

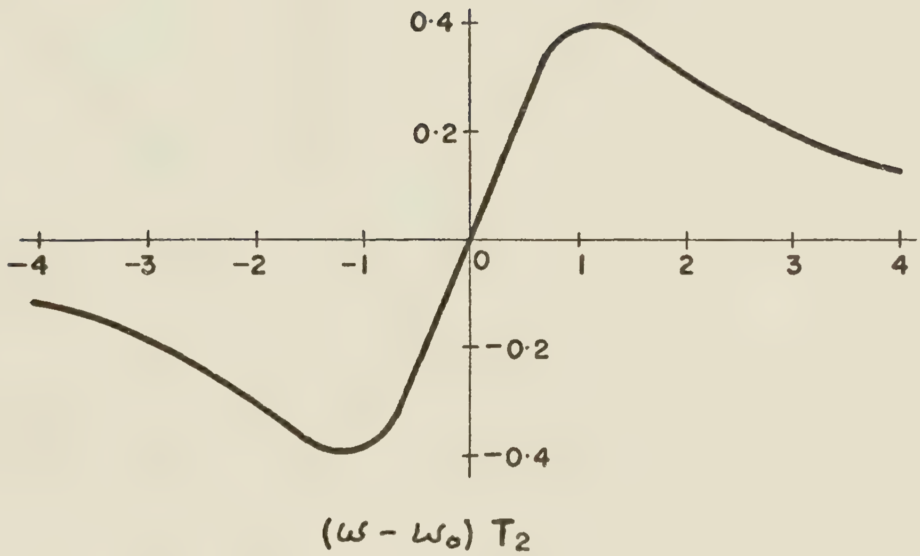

(b)

FIGURE 3: The absorption (a) and dispersive (b) components of the nuclear magnetization as a function of frequency.

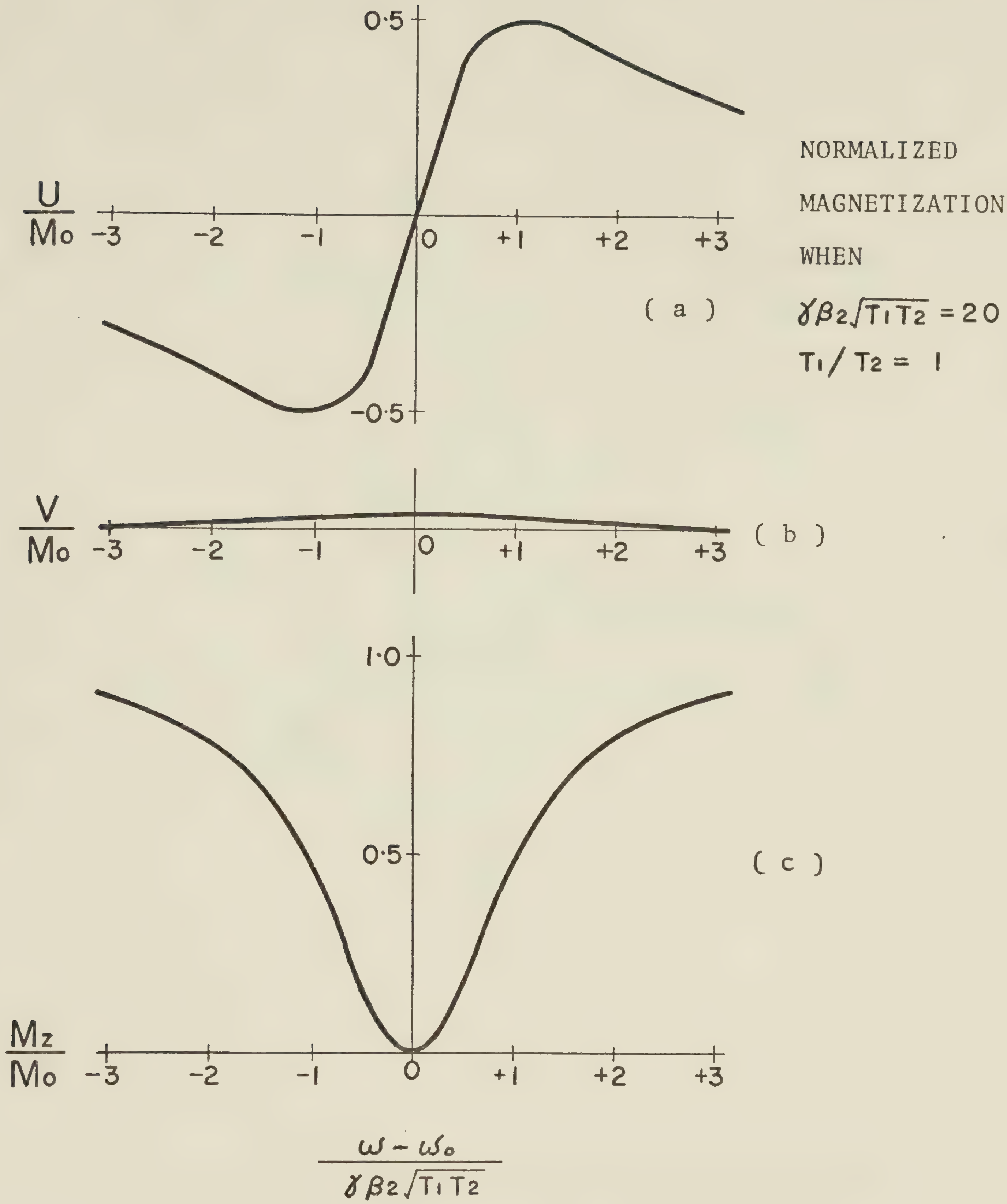

FIGURE 4: The dispersion (a), absorption (b) and z component (c) of the nuclear magnetization as a function of frequency when the saturation factor, $\gamma B_2\sqrt{T_1T_2}$, is larger than unity.

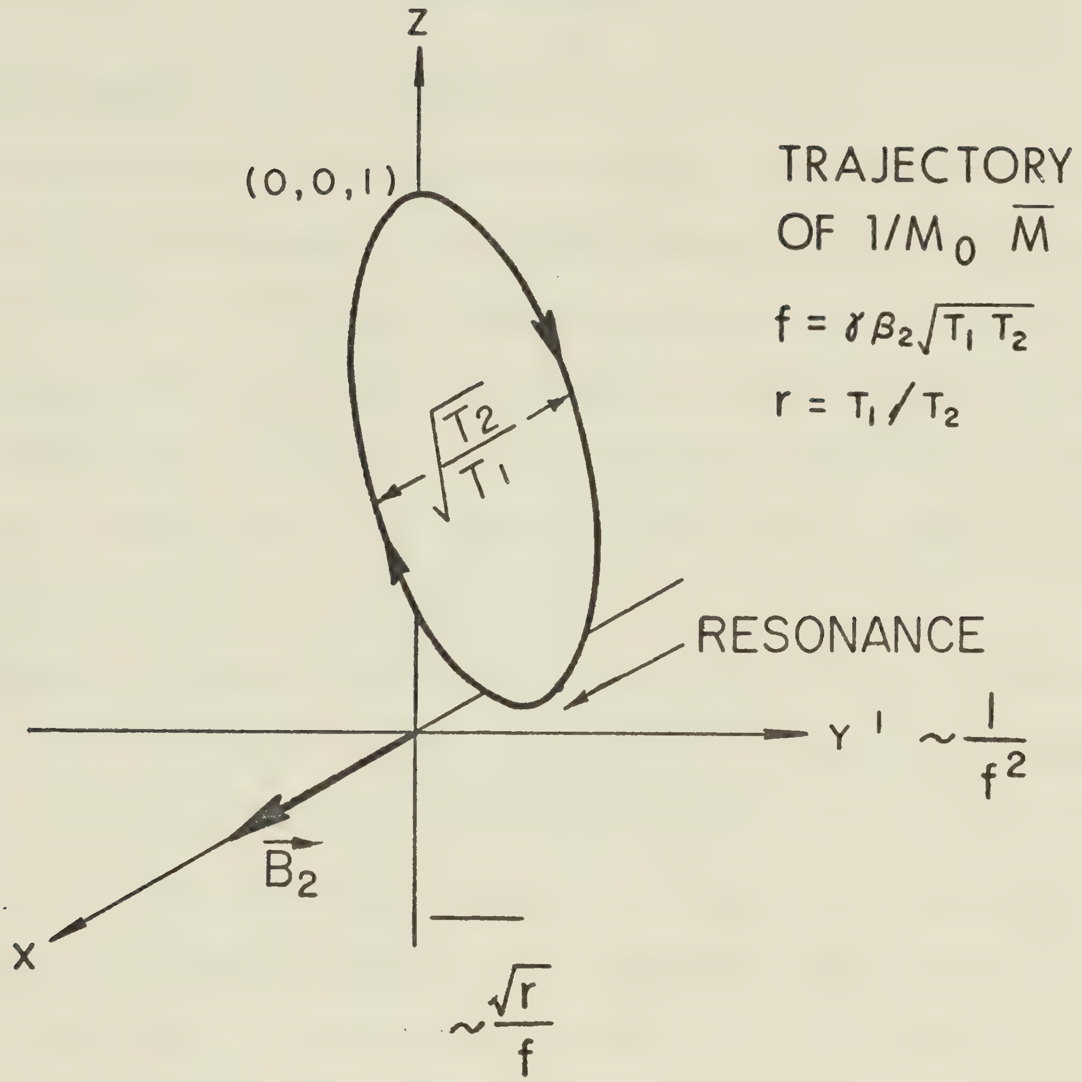

FIGURE 5: The trajectory of the magnetization as the magnetic field sweeps through resonance.

CHAPTER THREE

EXPERIMENTAL

Sample Purification and Preparation

1) Chloroform: Silanor (chloroform-d containing about 1% [V/V] tetramethylsilane (TMS) reference standard) was purchased from Merck Sharp & Dohme Canada Limited. Chloroform was added drop by drop to a sample of silanor until the two peaks were of roughly equal intensities. The sample was then degassed using five freeze - pump - thaw cycles.

2) Water: A sample of triply distilled water was adjusted to pH 11.5 with NaOH. It was transferred into a NMR capillary insert with deuterium oxide (D_2O), purchased from Columbia Organic Chemical Company, in the surrounding 2 mm sample tube as the external lock signal.

3) Adenosine 5'-Triphosphate (ATP): ATP (disodium salt) was obtained from Sigma Chemical Company. It was purified by dissolving it in a minimum amount of water, and passing it through a Chelex-100 column. The eluted solution was then freeze-dried. Enough D_2O and Ethylenediamine-tetraacetate acid (EDTA) were added to the purified ATP to prepare a 0.08 M ATP solution containing 2% EDTA as a mole fraction of the ATP concentration.

4) Adenylyl (3'→5') Adenosine (ApA): A-grade ApA was purchased from ICN Biochemical Company and was used without further purification. From its initial pH 3.2, it was adjusted to pH 7.2 with NaOD. Different concentration of ApA solutions were prepared in D_2O containing 2% EDTA. All samples were degassed in 5 mm NMR tubes (Wilmad) four times on a vacuum line before sealing.

5) Benzene: Spectral-grade benzene was obtained from Fisher Scientific Company. It was mixed with deutero-acetone and was degassed via five freeze - pump - thaw cycles.

6) *Ortho*-Dichlorobenzene: *o*-dichlorobenzene was purchased from Eastman Organic Chemical Company. A sample consisted of 90% *o*-dichlorobenzene and 10% deuteroacetone was prepared by mixing 1.8 ml. of *o*-dichlorobenzene and 0.2 ml. of deuteroacetone in a 10 mm NMR tube. The sample was degassed four times under vacuum.

Column Preparation

A Chelex-100 column with a 0.5 cm.^{2} x 28 cm. resin bed was made. Chelex-100 (Bio-Rad.) was treated with 1 N hydrochloric acid, 1 N sodium hydroxide and methanol and rinsed with triply distilled water after the acid and base treatment. The resin in the Na^+ form was then equilibrated with 0.05 M tri-hydroxymethyl-aminomethane (TRIS) (Schwartz-Mann) / 0.1 M potassium chloride (Fisher), pH = 7 (18).

To minimize the effect of paramagnetic impurities on the relaxation measurements, all the glassware (NMR tubes, storage containers, micropipets, etc.) used in these experiments was washed initially with soap and water. It was then immersed in concentrated nitric acid for at least five hours. All glassware was thoroughly rinsed with sufficient amount of distilled water. Finally it was rinsed by a solution of 0.1 M EDTA and 0.5 M sodium hydroxide.

All quoted pH values are uncorrected pH meter readings. For D_2O solutions, pD may be obtained by added 0.4 to the uncorrected pH values (19).

Proton Nuclear Magnetic Resonance Experiments

Proton chemical shifts, spin-lattice relaxation times, spin-spin relaxation times, calibration of the rf irradiating field as well as offset saturation experiments were measured in the Fourier transform mode at 100.0 MHz using the Varian HA-100-15 NMR spectrometer interfaced with the Digilab FTS/NMR-3 Fourier transform system including the FTS/NMR 400-z pulse unit and the Nova 1200 computer. The temperature was controlled to within 1°C using the Bruker B-ST 100/700 temperature controller.

The deuterium resonance from either D_2O or deuteroacetone ware used for the lock signal. Depending on the signal to noise ratio, 1 to 20 free induction decay signals were collected for each spectrum. The sweep width for each spectrum and the number of data points were chosen to give a resolution of 0.25 Hz per data point.

Spin-Lattice Relaxation Times

The spin-lattice relaxation times were measured using the (180° - τ - 90°) two pulse sequence. The 90° pulse width was 43 μsec.

Spin-Spin Relaxation Times

The spin-spin relaxation times were evaluated using the Carr-Purcell-Meiboom technique. The sources of error which may arise in the determination of spin-spin relaxation rates include a variety of constant pulse imperfections, inhomogeneity of the magnetic field, instabilities in pulse timing and effects of diffusion (6,12,13). These were minimized by satisfying the following conditions.

1) All pulse rotation parameters were kept within 5° of ideal Carr-Purcell-Meiboom conditions by keeping the time-base constant.
2) The resonance frequency did not change relative to the transmitter frequency by more than 1 - 2 Hz for at least a few hundred seconds.
3) Effects of diffusion through external field gradients were kept negligibly small by maintaining a constant non-spinning resolution as high as possible. The samples were not spun since the linewidths were better than 0.5 Hz.

The ability to reproduce Vold's degassed benzene T_2 value of twenty seconds (6) confirmed the accuracy of the spin-spin relaxation rates reported in this context.

Chemical Shift Measurements

The chemical shifts of the two adenine H-2 and the two adenine H-8 protons of ApA were calibrated with respect to TMS external reference.

Calibration of RF Irradiating Field

For the calibration of the rf irradiating field and offset saturation experiments, Hewlett-Parkard 5100 B external frequency synthesizer was used as the source of the rf irradiation. This was driven by a Hewlett-Parkard 5110 B synthesizer driver which in turn was driven by the 1 MHz output from the Digilab 10-94 synthesizer. This arrangement minimizes the relative frequency drift between the Digilab frequency synthesizer and the external synthesizer; it was less than 0.01 Hz over a period of six hours. The output of the HP 5100 B synthesizer was fed to a 230 A Boonton Radio Co. amplifier through a rf attenuator. Finally the output of the power amplifier was fed to the probe in parallel with the output of the Digilab 400-2 pulse unit.

For the measurement of the irradiating field, usually expressed in Hz as $\gamma B_2/2\pi$, the sharp isolated resonances of water or benzene were employed. The field was measured by the Baldeschwieler single spin double resonance method (20,21), which in favourable cases is capable of one or two percent precision.

First the sample was subjected to a strong rf irradiation of probe input power roughly 0.2 mW at a frequency

offset (ν_2-ν_o), typically 9 Hz away from the single resonance peak. This rf irradiation was maintained throughout the calibration. A single 90° pulse was then applied and the Fourier transform of the response was recorded. At least two spectra were recorded for each frequency offset ((ν_2-ν_o) and -(ν_2-ν_o)) and appropriate averages were taken.

A typical experimental spectrum of the calibration of rf irradiating field is shown in Figure 6. It consists of two transitions symmetrically placed on either side and inverted with respect to each other. The feature at the centre consists of a superposition of the Lorentzian absorption at $\omega_2 = \omega_o$ as well as a strong rf spike due to the steady state response.

The range of rf irradiating field used in all experiments was between 6 - 12 Hz in order to be safely within the range of limiting behaviour of the saturation factor required in the previous section. With the magnitude of $\gamma B_2/2\pi$ being 6 - 12 Hz, it is easy to measure $\gamma B_2/2\pi$ using Baldeschwieler's double resonance method by knowing the frequency offset ν_2-ν_o of the rf irradiation and the separation of the two transitions Δ (Hz). The value of B_2 can then be calculated using the equation,

$$(\frac{\Delta}{2})^2 = (\nu_2-\nu_o)^2 + (\gamma B_2/2\pi)^2 \qquad [19]$$

<u>Proton Offset Saturation Experiments</u>

The pulse sequence for the offset saturation experiment is shown below.

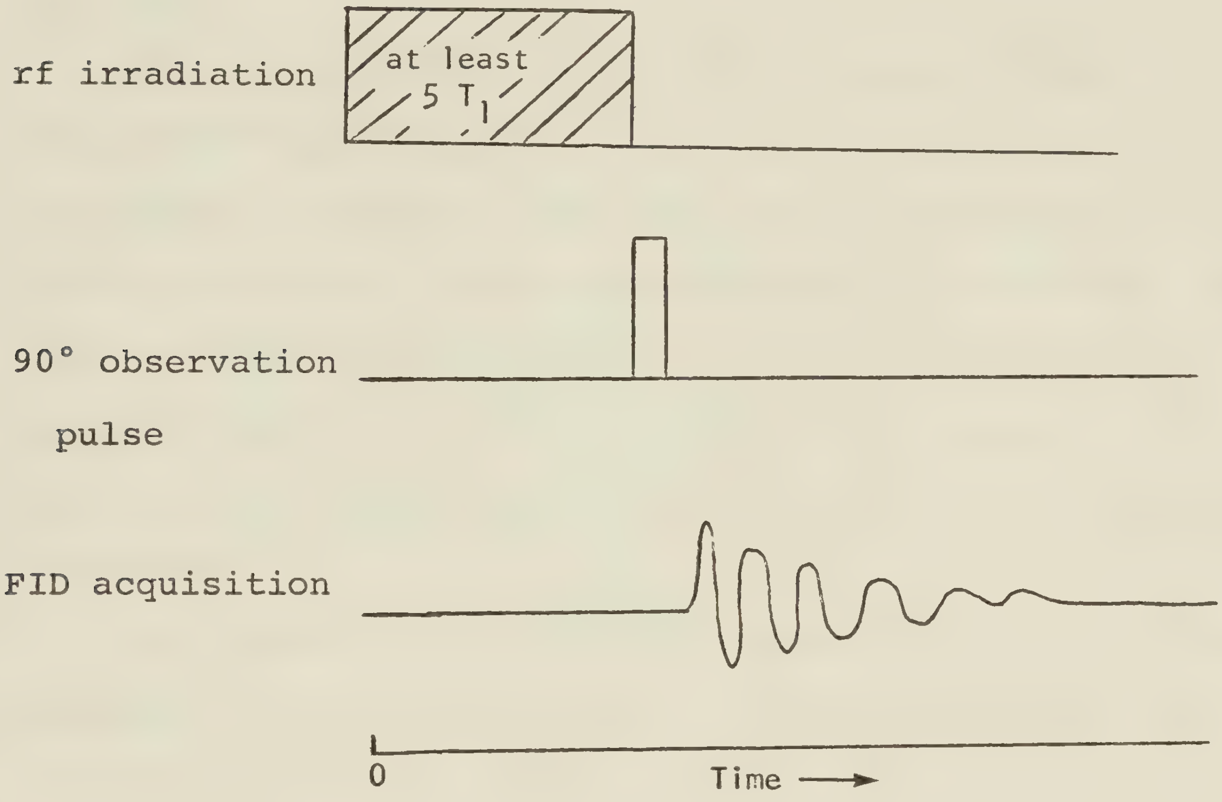

The spin system is equilibrated for an adequate time (about $5T_1$'s; on the order of a minute, usually) to achieve a steady state with respect to the strong rf irradiation at ν_2, displaced a few Hz, $\nu_2-\nu_o$ from resonance. The strong irradiation is shut off and a 90° analysis pulse is then applied, and the Fourier transform spectrum of the resulting free induction decay is obtained. In the course of a run

only the frequency offset, $\nu_2-\nu_o$, is varied to traverse the line of interest. All other parameters, including the strength of the irradiating field B_2, and all the characteristics of the analysis pulse and transform, are kept constant.

Figure 7 shows the results of a typical offset saturation experiment, in this case, for water at pH 11.5. The normalized z component shows the expected Lorentzian departure from unity in the neighbourhood of resonance. The analysis used only the points for which the normalized z component was in the range 0.3 to 0.7 for reasons to do with experimental precision; the full analysis is presented in Appendix 2.

The values of spin-lattice relaxation time, spin-spin relaxation time and the offset saturation experiment for the adjusted pH 11.5 water sample are tabulated in the following Table 1.

$^*T_1$	$= 3.57 \pm 0.21$ seconds
$^\dagger T_2$	$= 3.86 \pm 0.18$ second
$^\ddagger T_1/T_2$	$= 1.07 \pm 0.06$

*spin-lattice relaxation time obtained using (180° - τ -90°) pulse sequence

†spin-spin relaxation time obtained using Carr-Purcell -Meiboom technique

‡value obtained from the offset saturation experiment

Table 1 : ^{1}H T_1, T_2, and T_1/T_2 measurements of pH adjusted 11.5 water sample.

Meiboom (22) has shown that the spin-lattice and spin-spin relaxation times are essentially equal at pH greater than 9.5 for natural water (0.037% O^{17}). From Table 1, the deduced ratio T_1/T_2 is satisfactorily close to the expected value; it also accords with the relaxation times which were individually determined for this sample by standard methods.

Six determinations of the ratio T_1/T_2 for this water sample gave an average of 0.99 with a standard deviation 0.09. This is consistent with estimates of standard deviations estimated from an analysis of the experimental error in B_2, M_0 and M_z as shown in Appendix 2, which suggest precision of the order of 10 to 15 percent. This is essentially the state of the art for relaxation time measurements (2,14).

The following are some practical considerations which arose during the development of the technique:

1) The samples are not spun in order to avoid spinning side bands which might interfere with the calibration of the rf irradiating field B_2.
2) An alternative way of calibrating B_2 is to perform the offset saturation experiment, that is the one just described, on a sample whose relaxation time ratio is known. The pH 11.5 water resonance peak serves well for this purpose.

3) It is important to remember that the analysis is based on two assumptions that the magnetization is in fact showing limiting behaviour described by equation [20], and that one is in fact observing the z magnetization. The size of the saturation factor is important as shown in Figure 5. The residual v magnetization at resonance is of the order of $1/f$, where $f = \gamma B_2 \sqrt{T_1 T_2}$. The residual z magnetization and the departure of its value from the appropriate form, are both of the order of $1/f^2$. Clearly the saturation factor must be larger than 10 and preferably around 100 (Appendix 3). It turns out that, for reasonable relaxation times (of the order of a few seconds), such a saturation factor requires irradiating with a field, measured as $\gamma B_2/2\pi$, of only a few Hz. Such values are routinely available, since they are those used for homonuclear decoupling.

4) It is important to ensure that the analysis pulse is exactly 90 degrees. There are large u (and sometimes v) mode signals in the neighbourhood of resonance, where the z component that is measured is small; an inaccurate analysis pulse will mix the u mode signals with the signal that one wants to observe. It turns out that the approach of the observed signal to zero near resonance and the $(\Delta\nu^2)$ behaviour are a good test that both of the last two conditions have been fulfilled.

5) One must be careful about the phase of the FID transform with respect to the analysis pulse. Since the analysis signal at ν_1 is randomly phased with respect to the equilibrating field ν_2, the out of phase component of the transformed FID will contain an indeterminate mixture of u and remnant v mode signals. One may be able to discriminate satisfactorily against out of phase signals, because the phase relationships established in measuring M_0, with B_2 off, were stable throughout the run. With weak signals one may take advantage of the fact that the out of phase component, having random phase and odd parity, will tend to average to zero as FID's are accumulated. It would be better still if a short homospoil pulse were applied after B_2 is shut off and before the analysis pulse. Up to now our spectrometer does not yet have one.

6) In order to minimize the residual rf spike which might complicate the measurement of the z magnetization, the amount of coupling between the transmitter and the receiver coil has to be reduced by adjusting the mechanical leakage to a minimum.

7) One must be careful about the magnitude of the spin-lattice relaxation time of the resonance peak. Since the spin system needs a time period of $5T_1$'s to equilibrate in order to achieve a steady state with respect to the rf irradiation, if the value of T_1 is in the

order of 30 sec. or over, an instrumental limitation will be imposed on the offset saturation technique.

In most commercial NMR spectrometers, the maximum repetition time scale on the gated decoupling system only goes up to 99.9 seconds. This time scale limitation on most spectrometers in fact arose during the ^{13}C offset saturation experiment of *ortho*-dichlorobenzene. The spin-lattice relaxation times for the three carbon resonances of *ortho*-dichlorobenzene were measured. The T_1 value for <u>C</u>Cl (low-shielding line) was 128 ± 22 sec., <u>C</u>CCl was 9.28 ± 0.43 sec. and <u>C</u>CCCl (high-shielding line) was 8.02 ± 0.27 sec.. Using the offset saturation technique, the ratios T_1/T_2 were easily determined for carbons <u>C</u>CCl and <u>C</u>CCCl. However, it was not possible to determine ratio T_1/T_2 for carbon <u>C</u>Cl since one needs to equilibrate the spin system for a time period of over 600 seconds.

In order to overcome this instrumental limitation, one might install a larger time scale clock into the gated decoupling system.

^{13}Carbon Offset Saturation Experiments

^{13}C NMR spectra were taken with a Bruker HFX-90 NMR spectrometer operating at 25.2 MHz in the Fourier transform mode with noise decoupling of ^{1}H at 100 MHz. An external frequency synthesizer (HP 5100 B) is used as the source of the rf irradiation.

The pulse sequence for the ^{13}C offset saturation experiment is the same as for the ^{1}H offset saturation experiment, in addition, the noise decoupling of ^{1}H is maintained throughout the course of the experiment. The strong ^{13}C rf irradiating field is applied at a frequency offset $\nu_2-\nu_o$ with respect to the line of interest. After a steady state is achieved (in a time of at least $5T_1$), a 90° observation pulse is applied and the Fourier transform of the resulting FID is collected.

^{31}Phosphorus Nuclear Magnetic Resonance Experiments

^{31}P NMR spectra of ATP were obtained on a Bruker HFX-90 NMR spectrometer (36.4 MHz for ^{31}P) interfaced with a Nicolet 1085 computer. The proton decoupled FT spectra were recorded with a sweep width of 2000 Hz and 8K data points. The ^{31}P line-width at half-height of the α, β and γ ATP resonances were measured to ensure there was no line broadening due to paramagnetic impurities.

It was found that the ^{31}P line-widths at half-height varied between 1.5-3.0 Hz without EDTA. If EDTA was present, their line-widths at half-height were always less than 2.0 Hz.

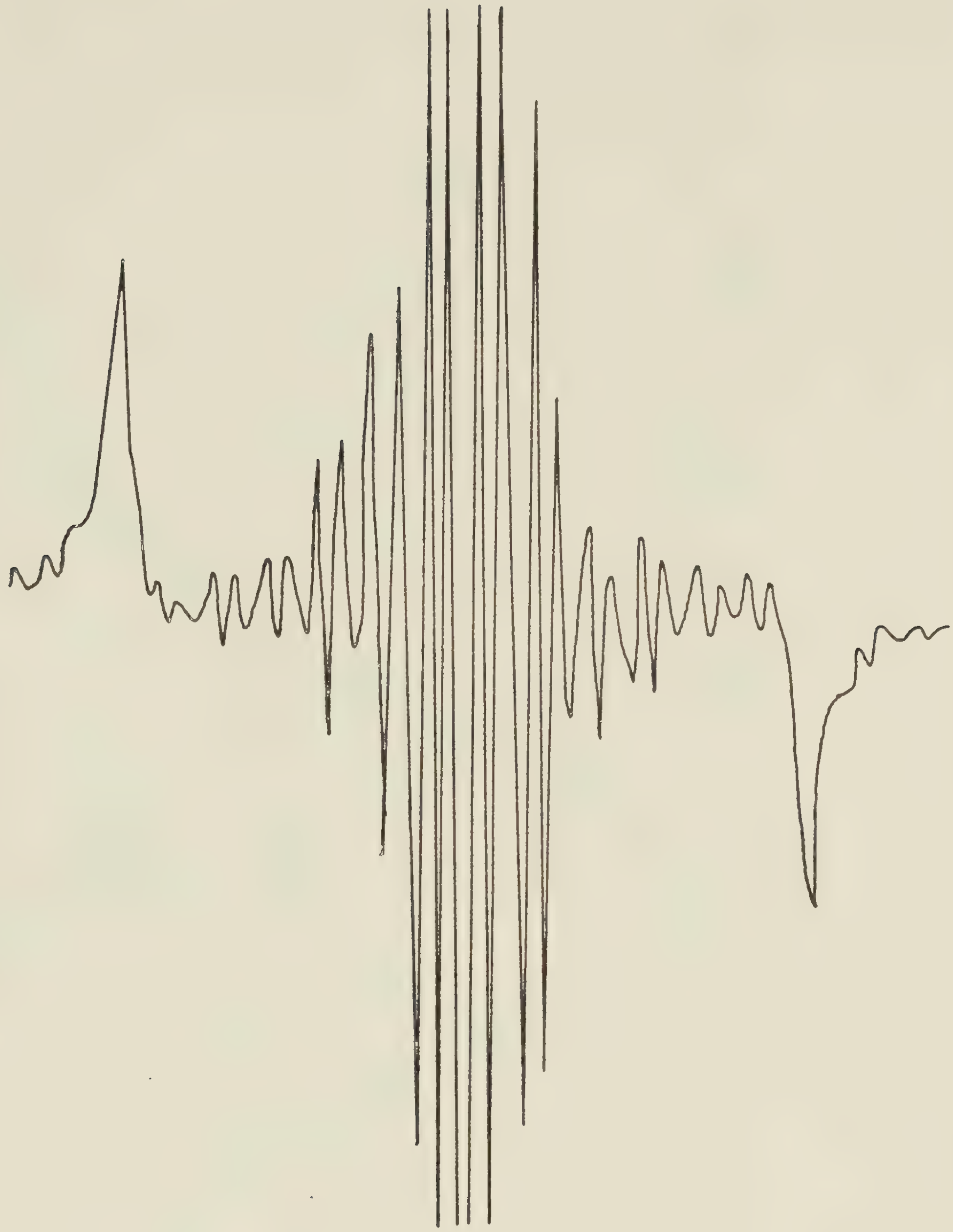

FIGURE 6: Typical experimental proton FT NMR spectrum of adjusted pH 11.5 water sample in the presence of a strong rf field in the Baldeschwieler's measurement of γB_2.

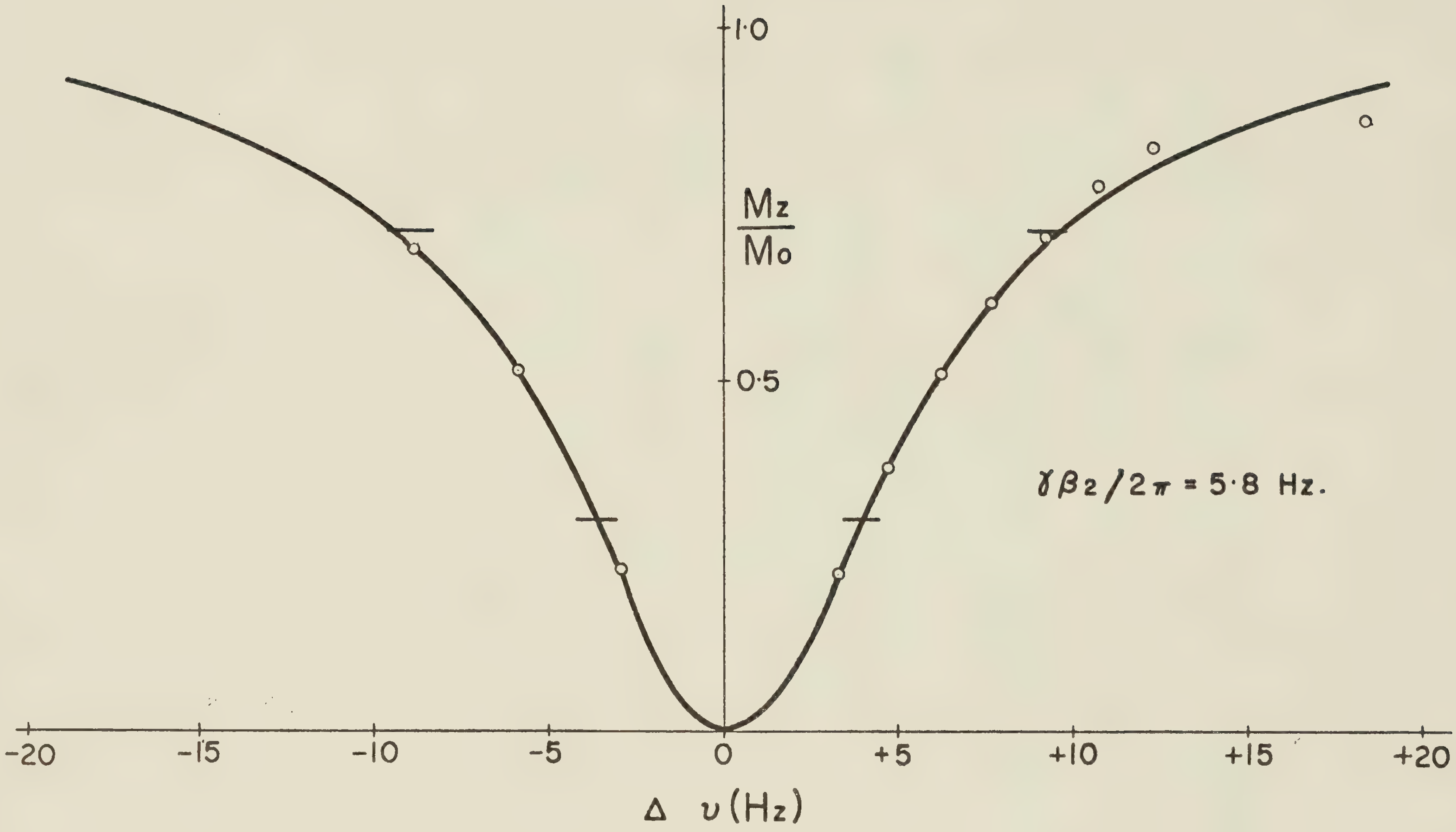

FIGURE 7: Results of a typical offset saturation experiment for adjusted pH 11.5 water sample.

CHAPTER FOUR

RESULTS & DISCUSSION

Least squares analysis was carried out on the data of all spin-lattice relaxation time measurements. T_1 was determined from the slope of a plot of $\ln(A_\infty - A_\tau)$ vs. τ, where A_τ is the initial amplitude of the FID following the 90° pulse at time τ, and A_∞ is the limiting value of A_τ for a very long interval between 180° and 90° pulses.

Water

The results for the adjusted pH 11.5 water samples were discussed in the previous section.

Chloroform

The spin-lattice and spin-spin relaxation times in chloroform have been studied by various workers (23,24,25). The results for the relaxation of the proton of chloroform, at a concentration of a few percent in deuterochloroform, is shown in Table 2.

*$T_1 = 201.7 \pm 10.0$ seconds
†$T_2 = 11.8 \pm 0.81$ seconds
‡$T_1/T_2 = 17.9 \pm 1.7$
*spin-lattice relaxation time obtained using ($180° - \tau - 90°$) pulse sequence
†spin-spin relaxation time obtained using Carr-Purcell -Meiboom technique
‡value obtained from the offset saturation experiment

Table 2: ^1H T_1, T_2, and T_1/T_2 measurements of the chloroform sample.

The relaxation is essentially all intramolecular (23). The dipole-dipole T_1 relaxation is very weak due to dilution of spins. The spin-spin relaxation time is shortened by scalar interaction with the quadrupole-relaxed chlorines. The ratio T_1/T_2 obtained from the offset saturation experiment was 17.9 ± 1.7 (Figure 8). The ratio of the directly measured relaxation times comes out at 17.1 ± 2.0, which is in good agreement with the ratio of 17.9 ± 1.7 obtained by the offset saturation experiment.

From the measured relaxation times, the coupling between the chloroform hydrogen and chlorine can be determined. The relaxation times of the spin I are given by (3),

$$(1/T_1)_I = DD + \frac{2A^2}{3} S(S+1) \frac{\tau_s}{1 + (\omega_I - \omega_S)^2 \tau_s^2} \qquad [21]$$

$$(1/T_2)_I = DD + \frac{A^2}{3} S(S+1) \{\frac{\tau_s}{1 + (\omega_I - \omega_S)^2 \tau_s^2}\} \qquad [22]$$

where

DD = the contribution to $1/T_1$ and $1/T_2$ from the dipolar coupling with the spins S.

A = spin-spin coupling constant

τ_s = the relaxation time of nucleus S.

ω_I, ω_S = resonance frequency of spin I and spin S.

The contribution from the DD term is the same for T_1 and T_2 and independent of the nuclear frequency because of the very short correlation time of the dipolar coupling (3). Subtracting equation [21] from [22] one obtains

$$(\frac{1}{T_2})_I - (\frac{1}{T_1})_I = \frac{1}{3} A^2 S\ (S+1)\ \tau_s \qquad [23]$$

With the value of the chlorine relaxation time $T_1(^{35}Cl)$ = 34 μsec. at 30°C (21), one can compute the value for the H-Cl coupling constant from equation [23].

The result is that

$$J_{H-Cl} = A/2\pi = 6.9 \text{ Hz}$$

This value is in agreement with that of Farrar and Becker (26), and nicely in the middle of the range (4 to 11 Hz) of reported values (23).

Adenosine 5'-Triphosphate

Adenosine 5'-triphosphate is one of the most important coenzymes and a major supplier of energy in most biological reactions and organisms (27,28). An ATP molecule consists of an adenine base, a ribose sugar and three phosphate groups (29). In aqueous solutions at neutral pH, most of the ATP molecules (about 80%) exist as tetravalent anions (ATP^{-4}), and the rest (about 20%) as $ATPH^{-3}$ with the terminal phosphate protonated (30). At physiological temperature, both anions are mainly in the *anti*-conformation in which the C-8 end of the adenine ring is facing the phosphate group (31,32).

The spin-lattice relaxation time and the ratio T_1/T_2 of ATP is shown in Figure 9. From the T_1 measurements, one can see that the proton H-8 in ATP is more strongly relaxed than proton H-2. This is due to its *anti*-conformation with proton H-8 close to a number of ribose hydrogens. The measured spin-lattice relaxation times are in excellent agreement with values reported by Lam and Kotowycz (33).

The ratios T_1/T_2 are similar, which is expected, since the two protons share the motion of the rigid ring to which they are both attached.

From the ratio T_1/T_2, one can evaluate the correlation time of the ATP molecule by considering the expressions for $1/T_1$ and $1/T_2$ for a system of like spins. It can be shown that (3)

$$1/T_1 = \frac{2\gamma_H^4\hbar^2\, I(I+1)}{5r^6}\left[\frac{\tau_c}{1+\omega_o^2\tau_c^2} + \frac{4\tau_c}{1+4\omega_o^2\tau_c^2}\right] \qquad [24]$$

$$1/T_2 = \frac{\gamma_H^4\hbar^2\, I(I+1)}{5r^6}\left[3\tau_c + \frac{5\tau_c}{1+\omega_o^2\tau_c^2} + \frac{2\tau_c}{1+4\omega_o^2\tau_c^2}\right] \qquad [25]$$

where

γ = magnetogyric ratio of proton

τ_c = average reorientational correlation time

I = spin quantum number

$\hbar$ = Planck's constant/2π

ω_o = $2\pi\nu_o$, resonance frequency

r = the distance between the nuclei

From equations [24] and [25] one can write,

$$T_1/T_2 = \frac{1}{2}\left\{\frac{3\tau_c + \dfrac{5\tau_c}{1+\omega_o^2\tau_c^2} + \dfrac{2\tau_c}{1+4\omega_o^2\tau_c^2}}{\dfrac{\tau_c}{1+\omega_o^2\tau_c^2} + \dfrac{4\tau_c}{1+4\omega_o^2\tau_c^2}}\right\} \qquad [26]$$

However, equation [26] can be written in a simplified form as,

$$T_1/T_2 \approx 1 + \omega_o^2\,\tau_c^2 \qquad [27]$$

When comparing these two equations, one finds only a maximum of 17% discrepancy between values obtained from the two separate equations in the range of ratios T_1/T_2 under consideration (Appendix 4), and so equation [27] gives a good first approximation, which can be refined using equation [26].

Using the ratios T_1/T_2 for the ATP molecules, the correlation times for H-2 and H-8 protons is 1.04×10^{-9} seconds at 25°C (34). The slightly lower ratio for H-2, which has a shorter correlation time, suggests that some intermolecular relaxation is taking place.

Adenylyl (3'→5') Adenosine

An investigation into the intramolecular base - stacking interaction of adenylyl (3'→5') adenosine was carried out. An ApA molecule consists of two adenine bases, two ribose sugars and one phosphate group as shown in Figure 10. Due to asymmetric esterification of the sugar moieties of the two nucleosides to the phosphate group (3'-v's 5'-), the two adenine rings of ApA are not geometrically equivalent. The proton spectrum of ApA (35) clearly indicates that the same protons (H-2 or H-8) on the two adenine rings are not magnetically equivalent.

It is well established that biological bases, nucleosides, and nucleotides associate extensively in aqueous solution, and that they interact principally via vertical stacking of the pyrimidine and purine rings. These interactions have been studied by vapour pressure osmometry (36,37,38), sedimentation equilibrium (39,40), and by proton magnetic resonance spectroscopy (41,42,43).

The spin-lattice relaxation times T_1, for protons H-8(5'), H-8(3'), H-2(5') and H-2(3') were measured as a function of ApA concentration at the temperatures 33°C and 5°C. These T_1 values are tabulated in Table 4.

In order to explain the relaxation data, four possible stacked conformations of ApA were constructed as shown in Figure 11. These illustrations of the various stacked

conformations are based on the molecular structure of the ApA molecule built from Dreiding models. In Figure 11, the conformations are viewed along the axis of the ribose - phosphate backbone in the direction of 5'-to 3'-phosphate esterification. The 3'-*anti*, 5'-*anti* conformation is designated by Fig. 11-a. The 3'-*anti*, 5'-*syn* (Fig. 11-b), 3'-*syn*, 5'-*anti* (Fig. 11-c) and 3'-*syn*, 5'-*syn* (Fig. 11-d) stacked conformations have been obtained by rotating either or both of the adenine rings 180° about the respective C_1'-N_9 glycosidic bond from the DNA-like base orientations.

From the spin-lattice relaxation times, one sees that both protons H-8 are more strongly relaxed than protons H-2 on the two adenine rings. Proton H-8(5') being the most strongly relaxed, will experience relaxation contributions from the ribose hydrogens of both 3' and 5' bases, only when the 5'-base is *anti*. Proton H-8(3') will experience intramolecular relaxation from the ribose hydrogens of 3'-base, only when the 3'-base is *anti*. A similar generalization can be made for the H-2 protons. Thus proton H-2(3') will experience a relaxation effect from the opposing 5'-base only when the 3'-base is *anti*. Proton H-2(5'), having the longest spin-lattice relaxation time, will be more exposed to the environment only when the 5'-base is *anti*. This clearly indicates that both adenine bases are preferentially oriented in the *anti* conformation relative to their respective furanose rings (Fig. 11-a).

This conformation is consistent with the studies of various workers based on chemical shifts (32,44,45), coupling constants (46) and optical activity investigations (47).

The spin-lattice relaxation times increase with a decrease in concentration. This is due to a decrease in the correlation time τ_c of ApA as the concentration decreases which in turn affects the spin-lattice relaxation times. By comparing the T_1 relaxation data at 33°C and 5°C, one finds that the T_1 values decrease due to increase in correlation time τ_c of ApA in going from a higher temperature to a lower one. The slowing down of the motion clearly indicate the stacking interaction between the two adenine rings increases at lower temperature.

ApA Offset Saturation Experiments

The ratios T_1/T_2 of the four adenine protons were obtained at different concentrations and temperatures using the offset saturation technique. The results are shown in Table 4.

The ratios T_1/T_2 for protons H-8 and H-2 of the two adenine rings can be measured in a single offset saturation run. The results are shown in Figure 12. The arrows show the points of irradiation among the four lines arising from the adenine protons of the dinucleotide ApA. The differences in T_1/T_2 between two temperatures again

reflect the increase in correlation time at lower temperature. As the concentration decreases the ratios T_1/T_2 decrease at both temperatures, which are consistent with a shorter correlation time.

The average reorientational correlation time τ_c of the four adenine protons was calculated from spin-lattice relaxation times as well as ratios T_1/T_2 for the four possible stacked conformers at 33°C and 5°C. The results are tabulated in Table 6, 7, 8 and 9.

The dipole-dipole contribution to $T_1^{-1}(i)$ for ^1H_i is given by (3)

$$T_1^{DD^{-1}}(i) = \frac{3}{2}\,\gamma_H^{\;4}\,\hbar^2 \sum_j r_{H_i\,H_j}^{\;\;-6}\,\tau_{c_{ij}} \qquad [28]$$

where

γ_H = magnetogyric ratio for ^1H

$r_{H_i\,H_j}$ = distance between the proton of interest (i) and proton (j)

$\tau_{c_{ij}}$ = the reorientational correlation time

The spin-lattice relaxation time provides a vehicle for the evaluation of the correlation time if the internuclear distance r is known. This scheme is averaging not r but rather raised to the minus six power, and hence, the method will only be applicable to interatomic distances

which are less than approximately 5 Å, the value beyond which the differential relaxation rate becomes insignificant. With this point in mind, the interatomic distances $r_{H_iH_j}$ of the four adenine ring protons were measured from the Dreiding model for the four possible stacked conformers. In constructing the Dreiding model of ApA, the two adenine rings were placed at least 3.4 Å apart (48).

The second approach to evaluate the correlation time is to use the approximate form of equation [26],

$$T_1/T_2 = 1 + \omega_o^2 \tau_c^2 \qquad [27]$$

Knowing the ratio T_1/T_2, the value of τ_c can be estimated.

One can make further conclusions about the stacked conformation of ApA by the comparison of τ_c values obtained from spin-lattice relaxation and T_1/T_2 data. Notably, the correlation times of proton H-2(5'), obtained from relaxation data at both different concentrations and temperatures, are in good agreement only when it is in 3'-*anti*, 5'-*anti* conformation. The difference in τ_c values obtained from the other three conformations may differ by as much as 20 times each other.

In order to show the sensitivity of the agreement of correlation time between the four possible conformations, the following index is used.

$$I = \frac{1}{N} \sum_{i=1}^{N} \left(\log \frac{\tau_{c_1}}{\tau_{c_2}} \right)^2 \qquad [28]$$

τ_{c_1} = the correlation time obtained from the offset saturation experiment

τ_{c_2} = the correlation time obtained from the spin-lattice relaxation time

N = the number of values of τ_{c_1}/τ_{c_2} used for each conformation

The indices for the overall four protons and for the proton H-2(5') only are presented in Table 3.

conformation	overall four protons I =	proton H-2(5')only I =
3'-anti, 5'-anti	0.11	0.048
3'-anti, 5'-syn	0.23	0.77
3'-syn, 5'-anti	0.15	0.17
3'-syn, 5'-syn	0.49	1.57

Table 3: Results of the sensitivity of the agreement of correlation time between the four possible conformations of ApA.

When all four protons are considered, the results favor the 3'-*anti*, 5'-*anti* conformation by a small amount. However, it is evident that proton H-2(5'), having the widest range of relaxation times affected by the conformation variation, and hence the most sensitive proton to conformational changes, is heavily in favor of the 3'-*anti*, 5'-*anti* conformation. Again, it is possible to conclude that the two adenine rings in ApA are stacked with each of the bases preferentially oriented in the DNA-like conformation (3'-*anti*, 5'-*anti*) relative to its ribose moiety.

The chemical shifts of the four adenine protons of ApA are plotted vs. the concentration at temperatures 33°C and 5°C in Figure 13 & 14. The effect of concentration on the spectrum of ApA has also been studied by Ts'o *et al* (32). Their basic observations are essentially in agreement with the results shown. The downfield shifts observed for all the proton resonances with decreasing concentration can be attributed to the breakdown of stacked intermolecular complexes.

^{13}Carbon Nuclear Magnetic Resonance Experiments

Carbon spin-lattice relaxation data are becoming increasingly used in chemistry. Carbon T_1 of individual resonances of high resolution NMR spectra may be determined via Fourier transformation fo the free induction signal excited by the (180° - τ - 90°) pulse sequence (49). The results provide information on molecular motion (50), and, in ^{13}Carbon spectroscopy with predominantly dipolar relaxation, about the number of directly attached protons (51).

The carbon spin-lattice and spin-spin relaxation times of benzene are known to be equal (52). The measured T_1 was 24.7 ± 0.17 seconds. Based on this information, the relaxation times of benzene is used to calibrate B_2 in the ^{13}C offset saturation experiment on the Bruker HFX-90 NMR spectrometer. The rf irradiating field was found to be 11.5 ± 0.5 Hz.

The ^{13}Carbon spectrum of *ortho*-dichlorobenzene was used to demonstrate the offset saturation technique. Incoherent off-resonance proton decoupling served to assign the three carbon resonances to $\underline{C}$Cl (low-shielding line), $\underline{C}$CCl, and $\underline{C}$CCCl (high-shielding line). Spin-lattice relaxation, measured by the inversion recovery technique, was very slow for $\underline{C}$Cl (T_1 = 128 ± 22 second), attributed to lack of directly bonded protons, and much faster for $\underline{C}$CCl (T_1 = 9.28 ± 0.43 second) and $\underline{C}$CCl (T_1 = 8.02 ± 0.27 second).

The relaxation times, T_1 and T_2, of the carbons of *ortho*-dichlorobenzene have been investigated (53). For the proton bearing carbons T_1 equals T_2 as expected, but for the chlorine bearing carbons T_1 is long, as proton dipole relaxation is relatively inefficient due to the increased distance between the nuclei. T_2 on the other hand is much shorter due to scalar relaxation with the quadrupolar chlorine nucleus.

Using the offset saturation technique, the ratio T_1/T_2 for $\underline{C}$CCl was 1.02 ± 0.04 and $\underline{C}$CCCl was 0.96 ± 0.07 so that their spin-lattice and spin-spin relaxation times are essentially equal.

Unfortunately, as was noted in the experimental section that it was not possible to determine ratio T_1/T_2 for carbon $\underline{C}$Cl due to instrumental limitation.

In conclusion, the application of the offset saturation technique in the measurement of relaxation in both proton and ^{13}Carbon Fourier transform NMR experiment have been demonstrated and discussed. One can appreciate the simplicity of this theory and the versatility of the offset saturation experiment.

Further work in this field could include the development of this technique in ^{31}P and ^{19}F NMR relaxation measurements. Future investigations into the validity of this technique in a coupled spin system and in mutually relaxing spin systems are also needed.

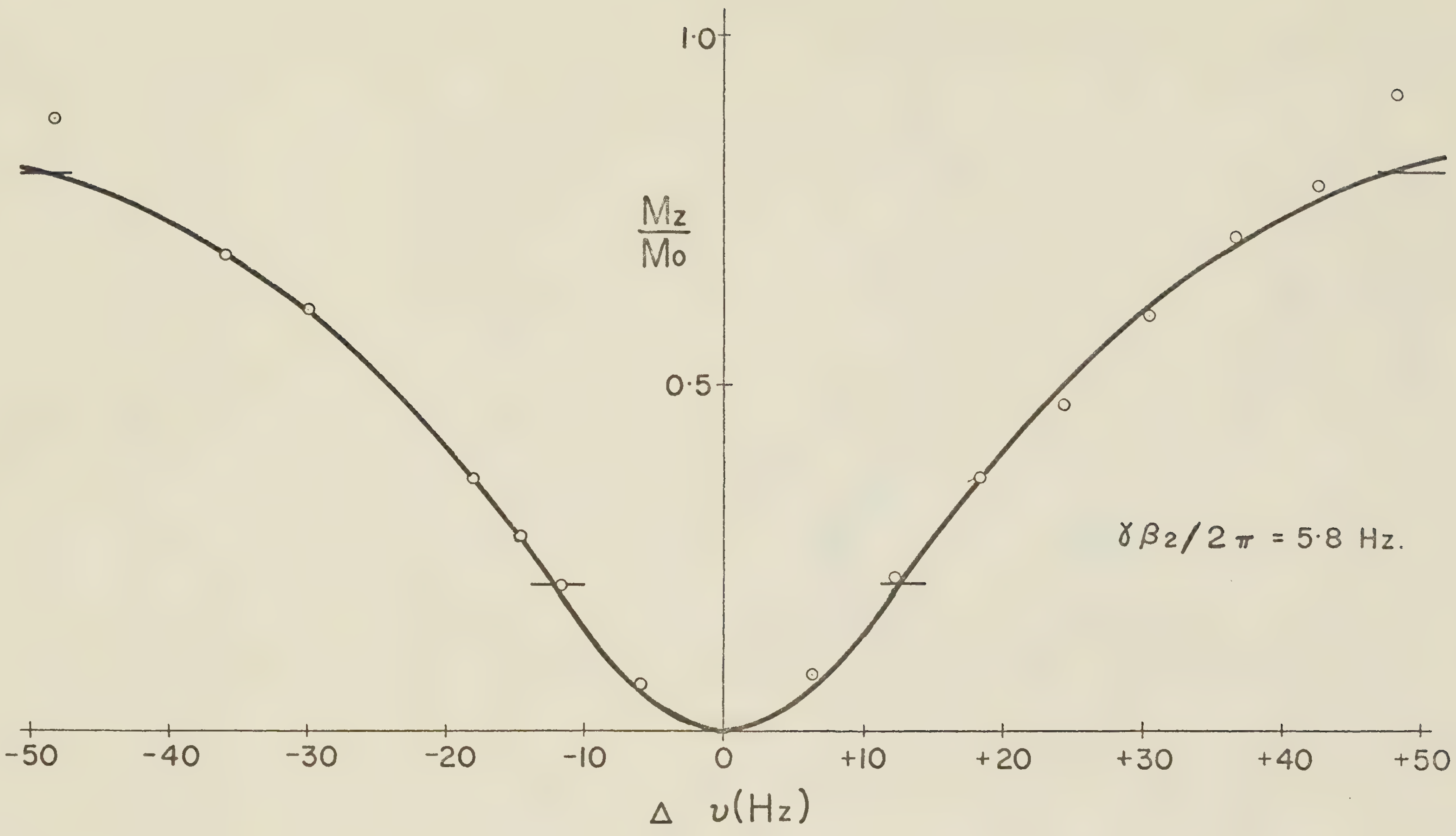

FIGURE 8: The result of the offset saturation experiment for the chloroform sample.

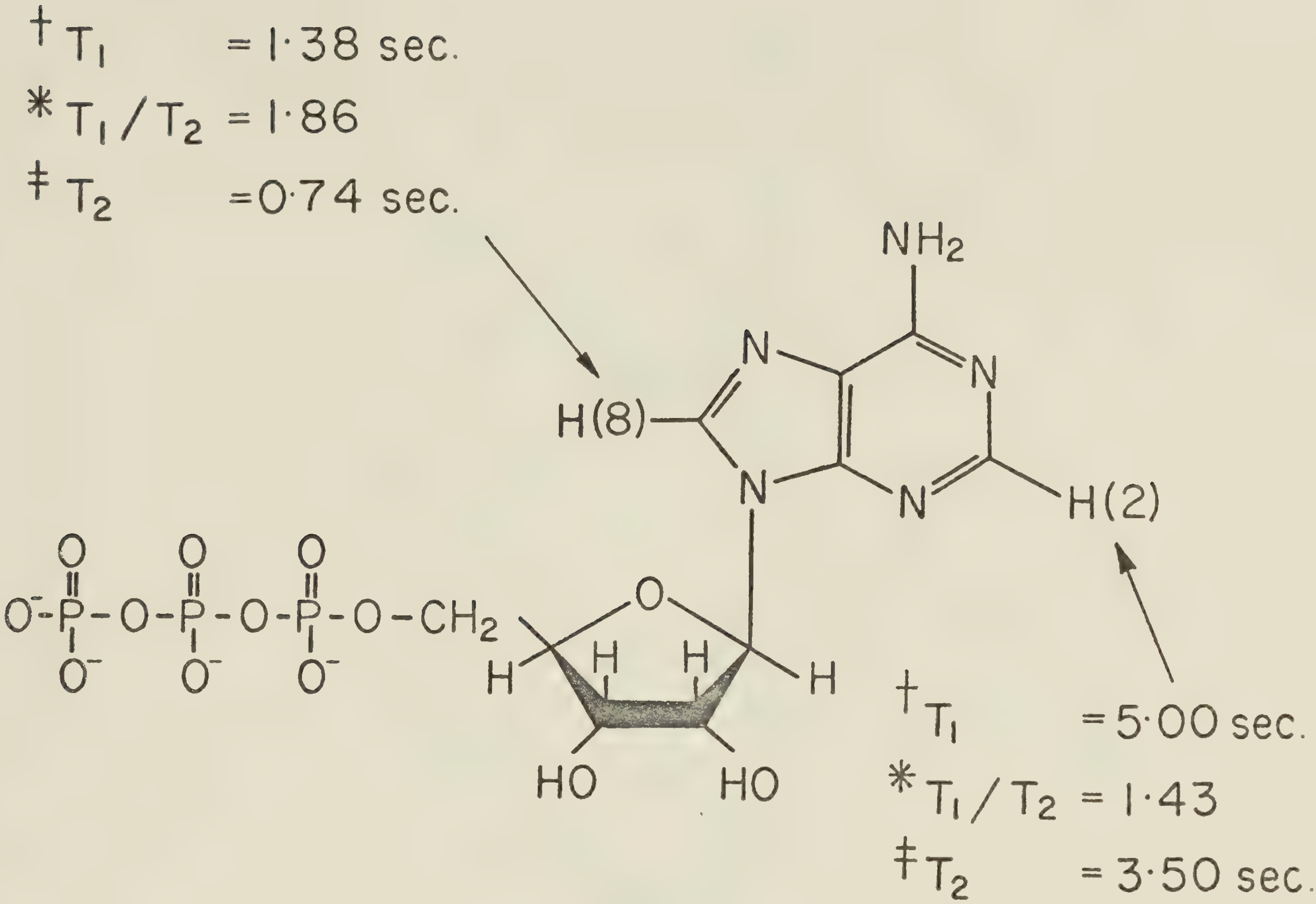

† T_1 obtained using ($180^0 - \tau - 90^0$) pulse sequence

* Value obtained from offset saturation experiment

‡ T_2 obtained using Carr-Purcell-Meiboom method

FIGURE 9: The spin-lattice, spin-spin relaxation times and ratio T_1/T_2 values of Adenosine 5'-triphosphate.

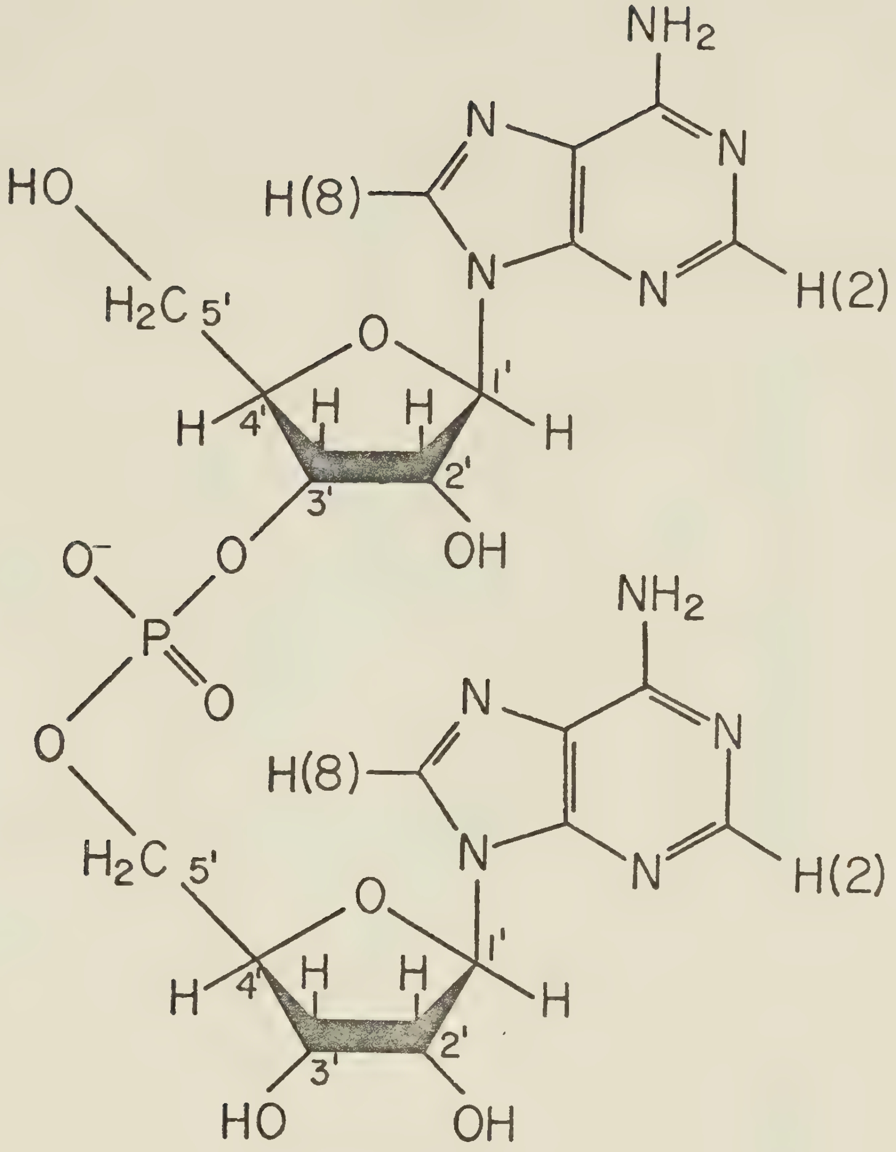

FIGURE 10: Adenylyl (3'→5') Adenosine (ApA)

Concentration (M)	H - 8(5')	H - 8(3')	H - 2(5')	H - 2(3')
0.1	0.65±0.02	0.82±0.02	3.31±0.13	2.93±0.13
0.06	0.69±0.02	0.85±0.03	3.93±0.12	3.64±0.12
0.04	0.79±0.03	1.09±0.04	4.96±0.30	4.43±0.24
0.02	0.92±0.03	1.33±0.06	6.85±0.03	5.96±0.16

(a)

Concentration (M)	H - 8(5')	H - 8(3')	H - 2(5')	H - 2(3')
0.1	0.34±0.02	0.50±0.02	1.54±0.08	1.45±0.06
0.06	0.37±0.02	0.53±0.02	1.97±0.08	1.64±0.06
0.04	0.36±0.01	0.51±0.03	2.07±0.06	1.74±0.07
0.02	-	0.53±0.05	2.41±0.22	1.98±0.14

(b)

All T_1 values are in units of seconds

TABLE 4: Spin-lattice relaxation time measurements for protons H-8(5'), H-8(3'), H-2(5') and H-2(3') of adenylyl (3'→5') adenosine as a function of concentration at temperatures (a) 33°C and (b) 5°C.

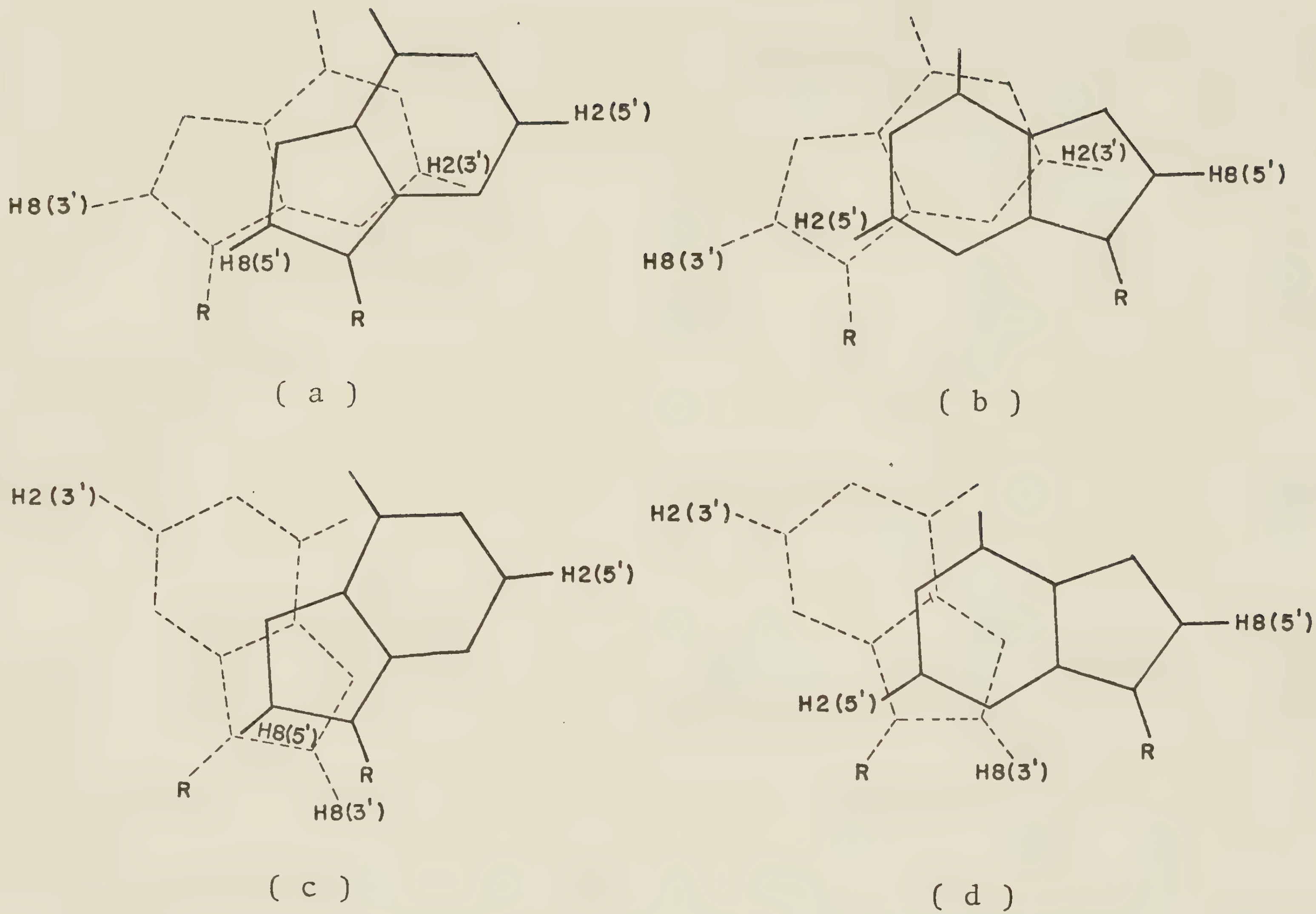

FIGURE 11: Four possible stacked conformers of Adenylyl (3'→5') Adenosine

Concentration (M)	H - 8(5')	H - 8(3')	H - 2(5')	H - 2(3')
0.1	1.21±0.08	1.17±0.09	1.26±0.16	1.21±0.14
0.06	1.04±0.12	1.03±0.08	1.12±0.17	1.20±0.13
0.04	1.00±0.15	1.01±0.06	1.06±0.18	1.14±0.16
0.02	-	1.01±0.27	1.04±0.12	1.17±0.12

(a)

Concentration (M)	H - 8(5')	H - 8(3')	H - 2(5')	H - 2(3')
0.1	1.69±0.18	1.44±0.04	1.51±0.13	1.63±0.11
0.06	1.43±0.08	1.35±0.04	1.40±0.11	1.33±0.05
0.04	1.15±0.13	1.23±0.08	1.28±0.12	1.20±0.04
0.02	-	1.03±0.04	1.22±0.16	1.16±0.16

(b)

TABLE 5: Ratios T_1/T_2 obtained from the offset saturation experiment for protons H-8(5'), H-8(3'), H-2(5') and H-2(3') of Adenylyl (3'→5') Adenosine as a function of concentration at temperatures (a) 33°C and (b) 5°C.

conc. (M)	temp.		conformation: 3'-anti,5'-anti $\tau_c \times 10^{10}$ sec.	3'-anti,5'-syn $\tau_c \times 10^{10}$ sec.	3'-syn,5'-anti $\tau_c \times 10^{10}$ sec.	3'-syn,5'-syn $\tau_c \times 10^{10}$ sec.
0.1	33°C	*	7.3	7.3	7.3	7.3
		ǂ	1.8	4.7	1.0	4.6
	5°C	*	13.2	13.2	13.2	13.2
		ǂ	3.5	8.9	2.0	3.0
0.06	33°C	*	3.2	3.2	3.2	3.2
		ǂ	1.7	4.4	1.0	4.4
	5°C	*	10.4	10.4	10.4	10.4
		ǂ	3.2	8.2	1.8	8.2
0.04	33°C	*	-	1.6	1.6	1.6
		ǂ	-	3.8	0.8	3.8
	5°C	*	6.2	6.2	6.2	6.2
		ǂ	3.3	8.4	1.8	8.4
0.02	33°C	*	-	1.6	1.6	1.6
		ǂ	-	3.3	0.7	3.3
	5°C	*	-	-	-	-
		ǂ	-	-	-	-

* τ_c calculated from ratio T_1/T_2 obtained by the offset saturation experiment. Probable error (excluding r^6 terms) Ca. $\pm$ 3 x 10^{-10} sec.

ǂ τ_c calculated from the spin-lattice relaxation times. Probable error (excluding r^6 term) Ca. $\pm$ 2 x 10^{-10} sec.

TABLE 6: The correlation time τ_c of proton H-8(5') for the four possible stacked conformers of ApA at 33°C and 5°C.

conc. (M)	temp.		conformation: 3'-anti,5'anti $\tau_c \times 10^{10}$ sec.	3'-anti,5'-syn $\tau_c \times 10^{10}$ sec.	3'-syn,5'-anti $\tau_c \times 10^{10}$ sec.	3'-syn,5'-syn $\tau_c \times 10^{10}$ sec.
0.1	33°C	*	6.6	6.6	6.6	6.6
		‡	1.6	2.8	3.2	2.4
	5°C	*	10.6	10.6	10.6	10.6
		‡	2.5	4.6	5.2	3.9
0.06	33°C	*	2.8	2.8	2.8	2.8
		‡	1.5	2.7	3.1	2.3
	5°C	*	9.4	9.4	9.4	9.4
		‡	2.4	4.3	4.9	3.7
0.04	33°C	*	1.6	1.6	1.6	1.6
		‡	1.2	2.1	2.4	1.8
	5°C	*	7.6	7.6	7.6	7.6
		‡	2.5	4.5	5.1	3.9
0.02	33°C	*	1.6	1.6	1.6	1.6
		‡	1.0	1.7	1.0	1.5
	5°C	*	2.8	2.8	2.8	2.8
		‡	2.4	4.3	4.9	3.7

* τ_c calculated from ratio T_1/T_2 obtained by the offset saturation experiment. Probable error (excluding r^6 term) Ca. 3×10^{-10} sec.

‡ τ_c calculated from the spin-lattice relaxation times. Probable error (excluding r^6 term) Ca. 2×10^{-10} sec.

TABLE 7: The correlation time τ_c of proton H-8(3') for the four possible stacked conformers of ApA at 33°C and 5°C.

conc. (M)	temp.		conformation 3'-anti,5'-anti $\tau_c \times 10^{10}$ sec.	3'-anti,5'-syn $\tau_c \times 10^{10}$ sec.	3'-syn,5'-anti $\tau_c \times 10^{10}$ sec.	3'-syn,5'-syn $\tau_c \times 10^{10}$ sec.
0.1	33°C	*	8.1	8.1	8.1	8.1
		ǂ	9.9	0.7	15.4	0.3
	5°C	*	11.4	11.4	11.4	11.4
		ǂ	21.3	1.5	33.0	0.7
0.06	33°C	*	5.5	5.5	5.5	5.5
		ǂ	8.3	0.6	13.0	0.3
	5°C	*	10.1	10.1	10.1	10.1
		ǂ	16.6	1.2	25.8	0.5
0.04	33°C	*	3.9	3.9	3.9	3.9
		ǂ	6.6	0.5	10.3	0.2
	5°C	*	8.4	8.4	8.4	8.4
		ǂ	15.8	1.2	24.6	0.8
0.02	33°C	*	3.2	3.2	3.2	3.2
		ǂ	4.8	0.4	7.4	0.2
	5°C	*	7.5	7.5	7.5	7.5
		ǂ	13.6	9.9	21.1	0.4

* τ_c calculated from ratio T_1/T_2 obtained by the offset saturation experiment. Probable error (excluding r^6 term) Ca. ± 3 x 10^{-10} sec.

ǂ τ_c calculated from the spin-lattice relaxation times. Probable error (excluding r^6 term) Ca. ± 2 x 10^{-10} sec.

TABLE 8: The correlation time τ_c of proton H-2(5') for the four possible stacked conformers of ApA at 33°C and 5°C.

conc. (M)	temp.		conformation 3'-anti,5'-anti $\tau_c \times 10^{10}$ sec.	3'-anti,5'-syn $\tau_c \times 10^{10}$ sec.	3'-syn,5'-anti $\tau_c \times 10^{10}$ sec.	3'-syn,5'-syn $\tau_c \times 10^{10}$ sec.
0.1	33°C	*	7.3	7.3	7.3	7.3
		‡	6.7	6.9	7.8	14.4
	5°C	*	12.3	12.3	12.3	12.3
		‡	13.4	13.9	15.7	61.1
0.06	33°C	*	7.1	7.1	7.1	7.1
		‡	5.4	5.5	6.3	11.6
	5°C	*	9.1	9.1	9.1	9.1
		‡	11.8	12.3	13.9	25.7
0.04	33°C	*	6.0	6.0	6.0	6.0
		‡	4.4	4.6	5.1	9.5
	5°C	*	7.1	7.1	7.1	7.1
		‡	11.2	11.6	13.3	24.2
0.02	33°C	*	6.6	6.6	6.6	6.6
		‡	3.3	3.4	3.8	7.1
	5°C	*	6.4	6.4	6.4	6.4
		‡	9.8	10.2	11.5	21.3

* τ_c calculated from ratio T_1/T_2 obtained by the offset saturation experiment. Probable error (excluding r^6 term) Ca. ± 3 x 10^{-10} sec.

‡ τ_c calculated from the spin-lattice relaxation time. Probable error (excluding r^6 term) Ca. ± 2 x 10^{-10} sec.

TABLE 9: The correlation time τ_c of proton H-2(3') for the four possible stacked conformers of ApA at 33°C and 5°C.

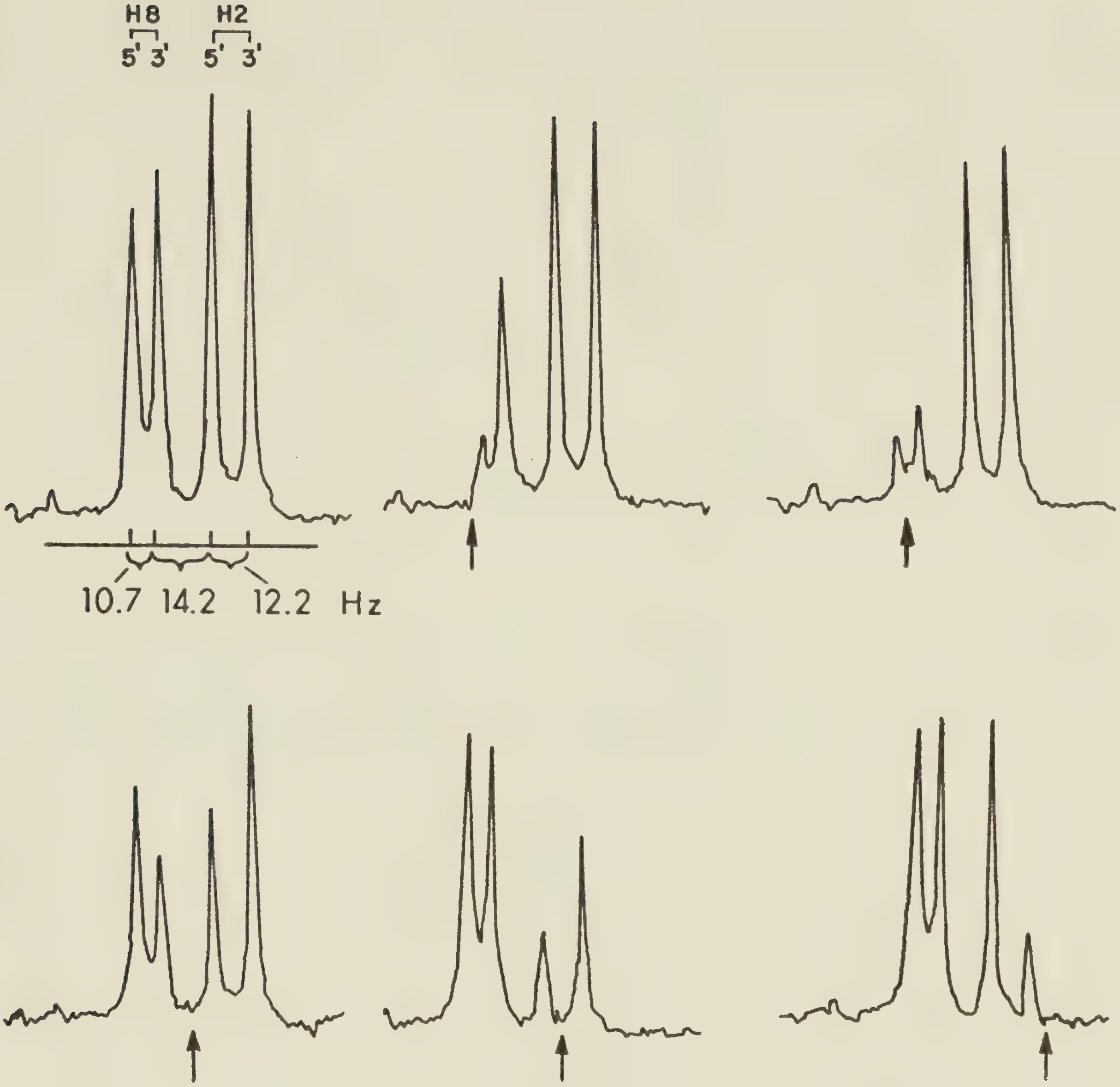

FIGURE 12: Typical proton FT NMR spectra of the four lines arising from the adenine protons of the Adenylyl (3'→5') Adenosine subjected to rf irradiation at the position marked.

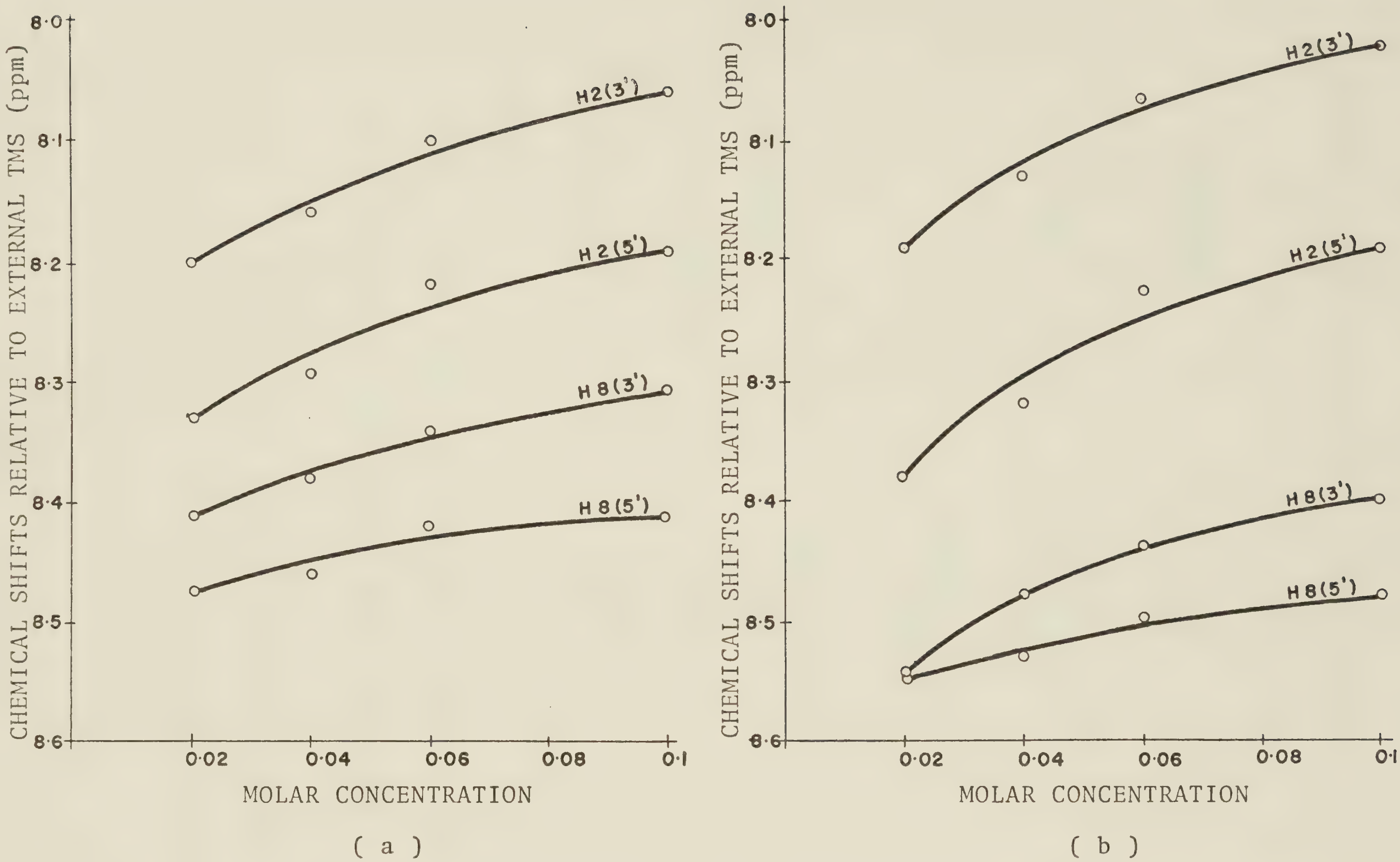

FIGURE 13: The concentration dependence of the chemical shifts of the four adenine protons of the Adenylyl (3'→5') Adenosine at temperatures (a) 33^{0}C and (b) 5^{0}C.

APPENDIX 1: Summary of nuclear relaxation mechanisms resulting from random molecular motion.

Mechanism	$\bar{b}^2_{loc}$
1. dipole - dipole a) nuclear - nuclear b) electron - nuclear	$\dfrac{(\gamma_I \gamma_S \hbar)^2 I(I+1)}{r_{IS}^{-6}}$
2. spin - rotation	$\dfrac{IkT(2C_{\perp}+C_{11})^2}{h^2}$
3. chemical shift anisotropy	$\gamma^2 B_o^2 (\sigma_{11}-\sigma_{\perp})^2$
4. scalar coupling	$\frac{2}{3}\, S(S+1)\ \pi^2 J^2$
5. quadrupolar	$(eq\, \frac{Q}{\hbar})^2$

where

b^2_{loc} = mean square average local magnetic field;

γ_I, γ_S = nuclear magnetogyric ratios of nuclei I and S;

$\hbar$ = Planck's constant / 2π;

$C_{\perp}, C_{11}$ = perpendicular and parallel spin rotation coupling constants;

$\sigma_{\perp}, \sigma_{11}$ = perpendicular and parallel shielding constants;

k = Boltzmann's constant;

r_{IS} = distance between nucleus I and nucleus S;

J = scalar coupling constant;

Q = quadrupole moment;

q = electric field gradient.

APPENDIX 2: The analysis of data for the offset saturation experiment.

The Bloch equation for the steady state z magnetization is,

$$M_z = M_o \frac{1 + T_2^2(\omega_o - \omega)^2}{1 + T_2^2(\omega_o - \omega)^2 + \gamma^2 B_2^2 T_1 T_2} \qquad [1]$$

In the event of $\gamma^2 B_2^2 T_1 T_2 >> 1$, equation [1] becomes

$$M_z/M_o = \frac{T_2^2(\omega_o - \omega)^2}{T_2^2(\omega_o - \omega)^2 + \gamma^2 B_2^2 T_1 T_2}$$

$$= \frac{1}{1 + \dfrac{(\gamma B_2)^2}{(\Delta\omega)^2} \dfrac{T_1}{T_2}} \qquad [2]$$

or

$$M_z/M_o = \frac{1}{1 + \dfrac{(\gamma B_2/2\pi)^2}{(\Delta\nu)^2} \dfrac{T_1}{T_2}} \qquad [3]$$

or

$$M_o/M_z = 1 + \frac{(\gamma B_2/2\pi)^2}{(\Delta\nu)^2} \frac{T_1}{T_2} \qquad [4]$$

$$= 1 + \frac{a}{\Delta^2} = Y \qquad [5]$$

where

$$\Delta = \nu - \nu_o = \Delta\nu$$

$$Y = M_o/M_z$$

$$a = (\gamma B_2/2\pi)^2 \frac{T_1}{T_2}$$

Rearranging equation [5],

$$\begin{aligned} a &= \Delta^2(M_o/M_z - 1) \\ &= \Delta^2(Y - 1) \end{aligned} \qquad [6]$$

One can evaluate $\Delta^2(Y-1)$ at each point and get a best mean value of a. Then

$$T_1/T_2 = \frac{a}{(\gamma B_2/2\pi)^2} \qquad [7]$$

The value of Y-1 outside the range 0.2 to 5.0 will contain large errors due to subtraction of near-equal numbers, and these values should not be included in the analysis.

A typical computer printout of data analysis for the offset saturation experiment is listed as follows:

ANALYSIS OF MZ/MO POINTS BETWEEN 0.20 and 0.80

GAMMAB2/(2*PI) = 5.8000 HZ

MO:- MEAN OF 4 DETERMINATIONS IS = 392.7500

STD. DEV. = 0.9574 (0.24%)

OFFSET(HZ)	MZ	MZ/MO	Y=MO/MZ	OFFSET**2*(2*Y-1)
0.0000	0.0000	0.0000		
3.0000	88.0000	0.2241	4.4631	31.1676
4.5000	150.0000	0.3819	2.6183	32.7712
6.0000	195.0000	0.4965	2.0141	36.5077
7.5000	238.0000	0.6060	1.6502	36.5743
9.0000	275.0000	0.7002	1.4282	34.6827
10.5000	305.0000	0.7766	1.2877	31.7194
12.0000	325.0000	0.8275	1.2085	30.0184
18.0000	340.0000	0.8657	1.1551	50.2675
24.0000	353.0000	0.8988	1.1126	64.8611
-3.0000	90.0000	0.2292	4.3639	30.2750
-6.0000	200.0000	0.5092	1.9637	34.6950
-9.0000	268.0000	0.6824	1.4655	37.7043
-12.0000	324.0000	0.8250	1.2122	30.5555
-18.0000	342.0000	0.8708	1.1484	48.0789

MEAN = 34.0108

STD. DEV. = 2.6503 (7.79%)

OFFSET(HZ)	MZ/MO(CALC)	MZ/MO(PRED)
3.0000	0.2241	0.2092
4.5000	0.3819	0.3732
6.0000	0.4965	0.5142
7.5000	0.6060	0.6232
9.0000	0.7002	0.7043
10.5000	0.7766	0.7642
12.0000	0.8275	0.8089
18.0000	0.8657	0.9050
24.0000	0.8988	0.9442
-3.0000	0.2292	0.2092
-6.0000	0.5092	0.5142
-9.0000	0.6824	0.7043
-12.0000	0.8250	0.8089
-18.0000	0.8708	0.9050

T1/T2 = 1.0110 STD. DEV. = 0.0788

APPENDIX 3: The effect of the magnitude of the saturation factor on the absorption, dispersion and z components of the nuclear magnetization.

The steady state Bloch equations are given by equations [11], [12] and [13]. In the event that the saturation factor, $\gamma B_2 \sqrt{T_1 T_2}$, is much large than unity, the z component of the magnetization is given by equation [14].

For $r = T_2/T_1 = 1, \quad f = \gamma B_2 \sqrt{T_1 T_2} = 5$

Δ	$U = \frac{5\Delta}{26+\Delta^2}$	$V = \frac{5}{26+\Delta^2}$	$Z = \frac{1+\Delta^2}{26+\Delta^2}$	$Z^1 = \frac{1}{1+\frac{25}{\Delta^2}}$
± 0.0	±0.0000	0.1923	0.0385	0.0000
± 0.5	±0.0476	0.1905	0.0476	0.0099
± 1.0	±0.1852	0.1852	0.0741	0.0385
± 1.5	±0.2655	0.0770	0.1150	0.0826
± 2.0	±0.3333	0.1667	0.1667	0.1379
± 3.0	±0.4286	0.1428	0.2857	0.2647
± 4.0	±0.4762	0.1190	0.4048	0.3902
± 5.0	±0.4902	0.0980	0.5098	0.5000
± 6.0	±0.4839	0.0806	0.5968	0.5902
± 8.0	±0.4444	0.0555	0.7222	0.7191
±12.0	±0.3529	0.0294	0.8529	0.8521
±16.0	±0.2837	0.0177	0.9113	0.9110

For $r = T_2/T_1 = 1$, $f = \gamma B_2 \sqrt{T_1 T_2} = 10$,

Δ	$U = \dfrac{10\Delta}{101+\Delta^2}$	$V = \dfrac{10}{101+\Delta^2}$	$Z = \dfrac{1+\Delta^2}{101+\Delta^2}$	$Z^1 = \dfrac{1}{1+\frac{100}{\Delta^2}}$
0	0.0000	0.0990	0.0099	0.0000
± 1	±0.0980	0.0980	0.0196	0.0099
± 2	±0.1905	0.0952	0.0476	0.0385
± 3	±0.2727	0.0909	0.0909	0.0826
± 4	±0.3419	0.0855	0.1453	0.1379
± 6	±0.4380	0.0730	0.2701	0.2647
± 8	±0.4848	0.0606	0.3939	0.3902
±10	±0.4975	0.0498	0.5025	0.5000
±12	±0.4898	0.0408	0.5918	0.5902
±16	±0.4482	0.0280	0.7199	0.7191
±24	±0.3545	0.0148	0.8523	0.8521
±32	±0.2844	0.0089	0.9111	0.9110

For $r = T_2/T_1 = 1$, $f = \gamma B_2 \sqrt{T_1 T_2} = 20$,

Δ	$U = \dfrac{200}{401+\Delta^2}$	$V = \dfrac{20}{401+\Delta^2}$	$Z = \dfrac{1+\Delta^2}{401+\Delta^2}$	$Z^1 = \dfrac{1}{1+\frac{400}{\Delta^2}}$
0	0.0000	0.0499	0.0025	0.0000
± 2	±0.0988	0.0494	0.0123	0.0099
± 4	±0.1918	0.0480	0.0480	0.0385
± 6	±0.2746	0.0458	0.0847	0.0826
± 8	±0.3441	0.0430	0.1398	0.1379
±12	±0.4404	0.0367	0.2661	0.2647
±16	±0.4871	0.0304	0.3912	0.3902
±20	±0.4994	0.0250	0.5006	0.5000

± 24	±0.4913	0.0205	0.5906	0.5902
± 32	±0.4491	0.0140	0.7193	0.7191
± 48	±0.3549	0.0074	0.8521	0.8521
± 64	±0.2846	0.0044	0.9111	0.9110
±128	±0.1525	0.0012	0.9762	0.9762
±256	±0.0776	0.0003	0.9939	0.9939

For $r = T_2/T_1 = 1$, $f = \gamma B_2 \sqrt{T_1 T_2} = 100$,

Δ	$U = \dfrac{100\Delta}{10001+\Delta^2}$	$V = \dfrac{100}{10001+\Delta^2}$	$Z = \dfrac{1+\Delta^2}{10001+\Delta^2}$	$Z = \dfrac{1}{1+\frac{10000}{\Delta^2}}$
0	0.0000	0.0100	0.0001	0.0000
± 2	±0.0200	0.0100	0.0005	0.0004
± 4	±0.0399	0.0100	0.0017	0.0016
± 8	±0.0795	0.0099	0.0065	0.0064
± 16	±0.1560	0.0097	0.0251	0.0250
± 32	±0.2902	0.0091	0.0930	0.0929
± 64	±0.4540	0.0071	0.2906	0.2906
± 96	±0.4996	0.0052	0.4796	0.4796
±128	±0.4851	0.0038	0.6210	0.6210
±256	±0.3389	0.0013	0.8676	0.8676
±384	±0.2439	0.0006	0.9365	0.9365

APPENDIX 4: The comparison of the ratio T_1/T_2 obtained from rigorous and approximate equations.

T_1/T_2 (true)	$\tau_c \times 10^{10}$ sec.	$^*T_1/T_2$ (approx.)
1.01	1.592	1.02
1.05	3.559	1.10
1.10	5.033	1.19
1.05	6.164	1.28
1.20	7.118	1.35
1.25	7.958	1.43
1.30	8.717	1.50
1.35	9.416	1.57
1.40	10.066	1.63
1.45	10.676	1.69
1.50	11.254	1.75
1.55	11.803	1.81
1.60	12.328	1.86
1.65	12.831	1.92
1.70	13.316	1.97
1.75	13.783	2.02
1.80	14.235	2.07
1.85	14.673	2.12
1.90	15.099	2.17
1.95	15.513	2.22
2.00	15.916	2.27

τ_c obtained from $\tau_c = \left(\frac{T_1/T_2 - 1}{\omega_o^2}\right)^{\frac{1}{2}}$

${}^{*}T_1/T_2$ values calculated using the equation

$$\frac{T_1}{T_2} = \frac{1}{2}\left\{\frac{3\,\tau_c + \frac{5\,\tau_c}{1+\omega_o^2\,\tau_c^2} + \frac{2\,\tau_c}{1+4\omega_o^2\,\tau_c^2}}{\frac{\tau_c}{1+\omega_o^2\,\tau_c^2} + \frac{4\,\tau_c}{1+4\omega_o^2\,\tau_c^2}}\right\}$$

BIBLIOGRAPHY

1. R. Freeman and H.D.W. Hill, J. Chem. Phys., 54, 3367 (1971).
2. R. Freeman and H.D.W. Hill, "Dynamic NMR Spectroscopy", (L.M. Jackman and F.A. Cotton, eds.), Chap. 5, Academic Press, 1975.
3. A. Abragam, "The Principle of Nuclear Magnetism", Oxford Univ. Press, London, 1961.
4. T.L. James, "Nuclear Magnetic Resonance in Biochemistry: Principles and Applications", Academic Press, New York, 1975.
5. R. Freeman and H.D.W. Hill, J. Chem. Phys., 55, 1985 (1971).
6. R.L. Vold, R.R. Vold and H.E. Simon, J. Magn. Resonance, 11, 283 (1973).
7. A.G. Redfield, Phys. Rev., 98, 1787 (1955).
8. I. Solomon, Compt. Rend. Acad. Sci., 248, 92; 249, 1631 (1959).
9. T.K. Leipert, J.H. Noggle, W.J. Freeman and O.L. Dalrymple, J. Magn. Resonance, 19, 208 (1975).
10. E.L. Hahn, Phys. Rev., 80, 580 (1950).
11. R. Freeman and H.D.W. Hill, J. Chem. Phys., 54, 301 (1971).
12. A. Allerhand, Rev. Sci. Instruments, 41, 269 (1970).
13. K.H. Weiss, Z. Instrumentenkunde, 75, 1 (1967).

14. D. Shaw, "Fourier Transform N.M.R. Spectroscopy", Chap. 10, Elsevier North-Holland Inc., New York, 1976.

15. F. Bloch. Phys. Rev., 70, 460 (1946).

16. R.K. Wangsness and F. Bloch, Phys. Rev., 81, 728 (1958).

17. D. Shaw, "Fourier Transform N.M.R. Spectroscopy", Chap. 3, Elsevier North-Holland Inc., New York, 1976.

18. O. Samuelson, "Ion Exchange Separations in Analytical Chemistry", 2nd Ed., Wiley, New York, 1963.

19. P.K. Glasoe and F.A. Long, J. Phys. Chem. 64, 188 (1960).

20. J.D. Baldeschwieler, J. Chem. Phys., 40, 459 (1964).

21. N.R. Krishna, J. Chem. Phys., 63, 4329 (1975).

22. S. Meiboom, J. Chem. Phys., 34, 375 (1961).

23. D. and M.T. Rogers, J. Chem Phys., 56, 542 (1972).

24. J.M. Winter, Compt. Rend, 249, 1346 (1959).

25. H. Ottavi, Compt. Rend, 252, 1439 (1961).

26. T.C. Farrar and E.D. Becker, "Pulse and Fourier Transform NMR", Chap. 4, Academic Press, 1971.

27. D.W. Hutchson, "Nucleotides and Coenzymes", John Wiley and Sons, New York, 1964.

28. S. Kit, "Metabolic Pathways", (D.M. Greenberg Editor), third ed., Vol. 4, Chap. 4, Acad. Press, New York, 1970.

29. A. Todd, Science, 127, 787 (1958).

30. R.M. Smith and R.A. Alberty, J. Chem. Phys., 60, 180 (1956).

31. S.S. Danyluk and F.E. Hruska, Biochemistry, 7, 1938 (1968).

32. M.P. Schweizer, A.D. Broom, P.O.P. Ts'o and D.P. Hollis, J. Amer. Chem. Soc., 90, 1042 (1968).

33. Y.F. Lam and G. Kotowycz, Can. J. Chem., 55, 3620 (1977).

34. F.F. Brown, I.D. Campbell, R. Henson, C.W.J. Hirst and R.E. Richards, European J. of Biochemistry, 38, 54 (1973).

35. P.O.P. Ts'o, N.S. Kondo, M.P. Schweizer and D.P. Hollis, Biochemistry 8, 997 (1969).

36. P.O.P. Ts'o, I.S. Melvin and A.C. Olson, J. Amer. Chem. Soc., 85, 1289 (1963).

37. P.O.P. Ts'o and S.I. Chan, J. Amer. Chem. Soc., 86, 4176 (1964).

38. A.D. Broom, M.P. Schweizer and P.O.P. Ts'o, J. Amer. Chem. Soc., 89, 3612 (1967).

39. K.E. Van Holde and G.P. Rossetti, Biochemistry, 6, 2189 (1967).

40. G.P. Rossetti and K.E. Van Holde, Biochem. Biophys. Res. Commun., 26, 717 (1967).

41. S.I. Chan, M.P. Schweizer, P.O.P. Ts'o and G.K. Helmkamp, J. Amer. Chem. Soc., 86, 4182 (1964).

42. O. Jardetzky, Biopolymers Symp., No. 1, 501 (1964).

43. M.P. Schweizer, S.I. Chan and P.O.P. Ts'o, J. Amer. Chem. Soc., 87, 5421 (1965).

44. S.I. Chan and J.H. Nelson, J. Amer. Chem. Soc., 91, 168 (1969).

45. T. Schleich, B.P. Cross and I.C.P. Smith, Nucleic Acids Research, 3, 355 (1976).

46. F.E. Evans, C. Lee and R.H. Sarma, Biochem. Biophys. Res. Commun., 63, 106 (1975).

47. C.A. Bush and I. Tinoco, Jr., J. Mol. Biol., 23, 981 (1967).

48. C. Giessner-Prettre and B. Pullman, J. Theor. Biol., 27, 341 (1970).

49. R.L. Vold, J.S. Waugh, M.P. Klein and D.E. Phelps, J. Chem. Phys., 48, 3831 (1968).

50. D. Doddrell and A. Allerhand, J. Amer. Chem. Soc., 93, 1558 (1971).

51. K.F. Kuhlmann, D.M. Grant and R.K. Harris, J. Chem. Phys., 52, 3439 (1970).

52. G.L. Levy and G.L. Nelson, "Carbon-13 Nuclear Magnetic Resonance for Organic Chemists", Wiley-Interscience, New York, 1972.

53. R. Freeman and H.D.W. Hill, J. Chem. Phys., 55, 1985 (1971).